

# **Evaluation of European air quality modelled by CAMx including the volatility basis set scheme**

**G. Ciarelli<sup>1</sup>, S. Aksoyoglu<sup>1</sup>, M. Crippa<sup>1,\*</sup>, J. L. Jimenez<sup>2,3</sup>, E. Nemitz<sup>4</sup>, K. Sellegri<sup>5</sup>,  
M. Äijälä<sup>6</sup>, S. Carbone<sup>7,\*\*</sup>, C. Mohr<sup>8</sup>, C. O'Dowd<sup>9</sup>, L. Poulain<sup>10</sup>, U. Baltensperger<sup>1</sup>,  
and A. S. H. Prévôt<sup>1</sup>**

[1]{Paul Scherrer Institute, Laboratory of Atmospheric Chemistry, 5232 Villigen PSI,  
Switzerland}

[2]{Cooperative Institute for Research in Environmental Sciences, University of Colorado,  
Boulder, CO 80309, USA}

[3]{Department of Chemistry and Biochemistry, University of Colorado, Boulder, CO 80309,  
USA}

[4]{Center for Ecology and Hydrology, Bush Estate, Penicuik, Midlothian, EH26 0QB, UK}

[5]{Laboratoire de Météorologie Physique CNRS UMR6016, Observatoire de Physique du  
Globe de Clermont-Ferrand, Université Blaise Pascal, 63171 Aubière, France}

[6]{University of Helsinki, Department of Physics, Helsinki, Finland}

[7]{Atmospheric Composition Research, Finnish Meteorological Institute, P.O. Box 503,  
00101 Helsinki, Finland}

[8]{Karlsruhe Institute of Technology, Institute of Meteorology and Climate Research,  
Germany}

[9]{School of Physics and Centre for Climate & Air Pollution Studies, Ryan Institute,  
National University of Ireland Galway, University Road, Galway, Ireland}

[10]{Leibniz-Institute for Tropospheric Research (TROPOS), Permoserstr. 15, 04318  
Leipzig, Germany}

[\*]{now at: Joint Research Centre, Institute for Environment and Sustainability, I-21020 Ispra  
(Va) JRC, Italy}

[\*\*]{now at: Institute of Physics, University of São Paulo, Rua do Matão Travessa R, 187,  
05508-090 São Paulo, S.P., Brazil}

Correspondence to: S. Aksoyoglu (sebnem.aksoyoglu@psi.ch)

## Abstract

Four periods of EMEP (European Monitoring and Evaluation Programme) intensive measurement campaigns (June 2006, January 2007, September-October 2008 and February-March 2009) were modelled using the regional air quality model CAMx with VBS (Volatility Basis Set) approach for the first time in Europe within the framework of the EURODELTA-III model intercomparison exercise. More detailed analysis and sensitivity tests were performed for the period of February-March 2009 and June 2006 to investigate the uncertainties in emissions as well as to improve the modelling of organic aerosols (OA). Model performance for selected gas phase species and PM<sub>2.5</sub> was evaluated using the European air quality database Airbase. Sulfur dioxide (SO<sub>2</sub>) and ozone (O<sub>3</sub>) were found to be overestimated for all the four periods with O<sub>3</sub> having the largest mean bias during June 2006 and January-February 2007 periods (8.9 ppb and 12.3 ppb mean biases, respectively). In contrast, nitrogen dioxide (NO<sub>2</sub>) and carbon monoxide (CO) were found to be underestimated for all the four periods. CAMx reproduced both total concentrations and monthly variations of PM<sub>2.5</sub> for all the four periods with average biases ranging from -2.1 µg m<sup>-3</sup> to 1.0 µg m<sup>-3</sup>. Comparisons with AMS (aerosol mass spectrometer) measurements at different sites in Europe during February-March 2009 showed that in general the model over-predicts the inorganic aerosol fraction and under-predicts the organic one, such that the good agreement for PM<sub>2.5</sub> is partly due to compensation of errors. The effect of the choice of volatility basis set scheme (VBS) on OA was investigated as well. Two sensitivity tests with volatility distributions based on previous chamber and ambient measurements data were performed. For February-March 2009 the chamber-case reduced the total OA concentrations by about 43% on average. On the other hand, a test based on ambient measurement data increased OA concentrations by about 47% for the same period bringing model and observations into better agreement. Comparison with the AMS data at the rural Swiss site Payerne in June 2006 shows no significant improvement in modelled OA concentration. Further sensitivity tests with increased biogenic and anthropogenic emissions suggest that OA in Payerne were affected by changes in emissions from residential heating during the February-March 2009 whereas it was more sensitive to biogenic precursors in June 2006.

## 1 Introduction

Air pollution is known to cause damage to human health, vegetation and ecosystems. It is one of the main environmental causes of premature death. Only in Europe, more than 400,000 premature deaths were estimated in 2011 with PM<sub>2.5</sub> (particles less than 2.5 µm in aerodynamic diameter) having the highest relative risk for health damage (WHO, 2014a). Air quality models help understanding the processes taking place between emission sources and pollutant concentrations at receptor sites. They are very useful to define control strategies for future legislation. In spite of large improvements in recent years, Chemical Transport Models (CTMs) have still some uncertainties (Solazzo et al., 2012a). Various air quality model intercomparison exercises were successfully carried out over the last decades to determine uncertainties in chemical and physical processes governing particulate matter and its precursors (Solazzo et al., 2012a; Bessagnet et al., 2014). However, a large variability in particulate matter concentrations was found between different models indicating process parameterization as one of the main reasons for such discrepancies. Moreover, recent studies based on AMS (Aerosol Mass Spectrometer) measurements at different sites in Europe, revealed that the organic fraction dominates the non-refractory PM<sub>1</sub> composition (Crippa et al., 2014). Organic aerosol (OA) can be found in the atmosphere from direct emission by various sources, such as fossil fuel combustion by road vehicle engines or residential wood combustion. Direct emissions of OA are typically referred to as primary organic aerosol (POA) whereas gas-to-particle conversion is referred to as secondary organic aerosol (SOA). Formation mechanisms of SOAs are not very well known yet and their representation in CTMs is still challenging (Hallquist et al. 2009; Fountoukis et al., 2011; Bergstrom et al., 2012; Li et al., 2013; Langmann et al., 2014; Tsigaridis et al., 2014). In one of our recent aerosol modelling studies we compared model PM<sub>2.5</sub> prediction with PM<sub>1</sub> AMS measurements for different sites (Payerne and Zürich) and periods (summer and winter) in Switzerland. We found that particulate matter was generally well reproduced by the model with the SOA fraction being under-predicted and POA over-predicted (Aksoyoglu et al., 2011). Traditional CTMs treat POA as non-volatile. Some studies however have revealed the semi-volatile nature of POA, through its dynamic equilibrium of organic aerosol with its gas phase, and the importance of semi-volatile (SVOC) and intermediate volatility (IVOC) organic compounds as SOA precursors (Donahue et al., 2006; Robinson et al., 2007; Cappa and Jimenez, 2010). To describe the absorptive partitioning and ongoing oxidation of the atmospheric material, a volatility basis set (VBS) where organic species are organized into

surrogates according to their volatility was developed (Donahue et al., 2011, 2012a,b). Air quality models updated with VBS scheme started being used (Lane et al., 2008; Murphy and Pandis, 2009; Hodzic et al., 2010; Fountoukis et al., 2011; Bergström et al., 2012; Murphy et al., 2012; Jo et al., 2013; Zhang et al., 2013; Athanasopoulou et al., 2013; Fountoukis et al., 2014). Bergström et al. (2012) reported an EMEP model study over Europe for the 2002-2007 period using different assumptions regarding partitioning and aging processes. They could not reproduce the measured OA levels in winter suggesting that residential wood combustion inventories might be underestimated in different parts of Europe. Fountoukis et al. (2014) applied the PMCAMx model to simulate EUCAARI (Kulmala et al., 2009, 2011) and EMEP (Tørseth et al., 2012) campaigns in Europe. They could reproduce most of PM<sub>1</sub> daily average OA observations within a factor of two, with the February-March 2009 period having the largest discrepancies. Zhang et al. (2013) deployed the CHIMERE model with the VBS framework during the MEGAPOLI summer campaign in the Greater Paris region for July 2009. They found a considerable improvement in predicted SOA concentrations which might be even overestimated depending on the emission inventory used. In our study, we applied the regional air quality model CAMx with the VBS scheme for the first time in Europe within the framework of EURODELTA-III model intercomparison exercise. In addition to the base case configuration used in the exercise, more sensitivity tests with the VBS scheme for winter and summer episodes were performed together with a general evaluation of the four EMEP field measurement campaigns.

## **2 Method**

### **2.1 The EURODELTA-III exercise**

The EURODELTA-III (EDIII) framework is a European model intercomparison exercise between several modelling teams sharing both efforts and technical knowledge in order to reduce model uncertainties and to improve understanding of the performances. It contributes to the scientific work of the United Nations Economic Commission for Europe (UNECE) Task Force on Measurement and Modelling (TFMM) within the Convention on Long-range Transboundary Air Pollution (CLRTAP). In the first phase of the EDIII exercise, 4 periods of the EMEP field measurement campaigns were chosen in order to evaluate the model results:

- 1 June – 30 June 2006
- 8 January – 4 February 2007
- 17 September – 15 October 2008

- 25 February – 26 March 2009

Multiple models were applied on a common domain and driven with the same input data provided by the National Institute for Industrial Environment and Risks (INERIS). However, for some models, different meteorology, boundary conditions and emissions data such as biogenic emissions were used (Bessagnet et al., 2014).

## **2.2 Modelling method**

### **2.2.1 CAMx**

The Comprehensive Air quality Model with extensions, CAMx-VBS (CAMx5.41\_VBS, kindly provided by ENVIRON before its public release) was used in this study. The model domain consisted of one grid with a horizontal resolution of  $0.25^{\circ} \times 0.25^{\circ}$ . The latitude and longitude grid extended from  $25.125^{\circ}\text{W}$  to  $45.125^{\circ}\text{E}$  and  $29.875^{\circ}\text{N}$  to  $70.125^{\circ}\text{N}$  resulting in  $281 \times 161$  grid cells covering the whole of Europe. Hourly four-dimensional meteorological fields for wind speed and direction, pressure, temperature, specific humidity, cloud cover and rain required by CAMx simulations were calculated from ECMWF IFS (Integrated Forecast System) data at  $0.2^{\circ}$  resolution. Vertical diffusivity coefficients were estimated following the Kz approach of O'Brien (1970) using PBL depth profiles as available in IFS data. CAMx simulations used 33 terrain-following  $\sigma$ -levels up to about 8000 m above ground level, as in the original IFS data. The lowest layer was about 20 m thick. MACC (Monitoring Atmospheric Composition and Climate) reanalysis data were used to initialize initial and the boundary condition fields (Benedetti et al., 2009; Inness et al., 2013). Elemental carbon, organic aerosol, dust and sulfate were used to model aerosol species at the boundaries of the domain. One half of the OA was assumed to be secondary organic aerosol (SOA) and the other half primary organic aerosol (POA), as recommended in the EDIII exercise. Photolysis rate inputs were calculated using the TUV radiative transfer and photolysis model (Madronich, 2002). The required ozone column densities to determine the spatial and temporal variation of the photolysis rates were extracted from TOMS data (NASA/GSFC, 2005). Removal processes as dry and wet deposition were simulated using the Zhang resistance model (Zhang et al., 2003) and a scavenging model approach for both gases and aerosols (ENVIRON, 2011), respectively. For the gas phase chemistry the Carbon Bond (CB05) mechanism (Yarwood et al., 2005) with 156 reactions and up to 89 species was used.

Partitioning of inorganic aerosols (sulfate, nitrate, ammonium, sodium and chloride) was performed using the ISORROPIA thermodynamic model (Nenes et al., 1998). Aqueous sulfate and nitrate formation in cloud water was simulated as well using the RADM aqueous chemistry algorithm (Chang et al., 1987).

## **2.2.2 Emissions**

### **Anthropogenic emissions**

Annual total gridded anthropogenic emissions were prepared and provided by INERIS for the EDIII exercise, which is based on a merging process of data-bases from different sources, i.e. TNO-MACC (Kuenen et al., 2011), EMEP (Vestreng et al., 2007), GAINS (The Greenhouse Gas and Air Pollution Interactions and Synergies). For specific countries where TNO-MACC emissions were missing (Iceland, Liechtenstein, Malta and Asian countries), the EMEP  $0.5^\circ \times 0.5^\circ$  emissions were used and re-gridded using adequate proxies such as “artificial land-use” and EPER (European Pollutant Emission Register) data (<http://www.eea.europa.eu/>) for industries. Total primary particle emissions were made available by EMEP in two different size ranges: below  $2.5\mu\text{m}$  (fine) and between  $2.5\mu\text{m}$  and  $10\mu\text{m}$  (coarse). Total emissions were later split to estimate the amount of elemental carbon, and organic matter for each of the 10 SNAP codes (Selected Nomenclature for Air Pollution) and country. The final emission inventory thus compiled consisted of 6 gas species namely methane, carbon monoxide, ammonia, sulfur oxides, non-methane volatile organic compounds and nitrogen oxides and 6 categories of particulate matter classes: fine elemental carbon (EC2.5), coarse elemental carbon (EC10), fine primary organic material (fine POA), coarse primary organic material (coarse POA), fine other primary particulate material (non-carbonaceous) and coarse other primary particulate material (non-carbonaceous).  $\text{PM}_{2.5}$  and  $\text{PM}_{10}$  emissions were provided by EMEP and they were split to elemental carbon and organic matter using the fractions given by IIASA (International Institute for Applied Systems Analysis) for each source and country. Total non-methane volatile organic compounds were split for the CB05 mechanism using the recommendations of Passant (2002). Hourly, weekly and monthly time profiles as in the EURODELTAII exercise were applied to total annual anthropogenic emissions.

## 187 **Biogenic emissions**

188 Biogenic VOC emissions were calculated using the Model of Emissions of Gases and  
189 Aerosols from Nature MEGANv2.1 (Guenther et al., 2012). This model is driven by  
190 meteorological variables such as hourly temperature, solar radiation, humidity, wind speed,  
191 soil moisture and land cover data including leaf area index (LAI) and plant function type  
192 (PFT) as available in the Community Land Model 4.0. 8-Days average satellite data at  $0.25^\circ \times$   
193  $0.25^\circ$  resolution were pre-processed and made available from the TERRA/MODIS satellite  
194 system. Sixteen plant function types including needle-leaved evergreen, needle-leaved  
195 deciduous, broad-leaved evergreen, broad-leaved deciduous, grass and crop for different  
196 climatic zones were prepared for this study at  $0.25^\circ \times 0.25^\circ$  resolution together with the global  
197 emission factors of  $\alpha$ -pinene,  $\beta$ -pinene, 3-carene, isoprene, limonene, 232-methylbutenol,  
198 myrcene,  $\text{NO}_x$ , *t*- $\beta$ -ocimene and sabinene. Common BVOC species such as isoprene, terpene,  
199 sesquiterpene, xylene and toluene were obtained for each hour and cell in the domain.

### 200 **2.2.3 VBS scheme**

201 A new volatility basis set (VBS) scheme is available in the CAMx model to describe changes  
202 in oxidation state and volatility. A total of four basis set simulates the evolution of organic  
203 aerosol in the atmosphere (Koo et al., 2014). POA emissions were split in HOA-like and  
204 BBOA-like emissions and allocated in two different basis sets. HOA-like emissions include  
205 emissions from all SNAP sectors except SNAP2 (non-industrial combustion plants) and  
206 SNAP10 (agriculture) which were assigned to BBOA-like emissions. Two other sets were  
207 used in the model to allocate secondary organic aerosol from anthropogenic (i.e. xylene and  
208 toluene) (ASOA) and biogenic (i.e. isoprene, monoterpene and sesquiterpene) (BSOA)  
209 gaseous precursors. These two sets also allocate oxidation products of POA vapours, from  
210 each of the two primary sets (HOA-like and BBOA-like). The 2D volatility space retrieved by  
211 Donahue et al. (2011; 2012a,b) was used to distribute the organic molecular structures for  
212 each of the volatility bins and different sets (Table S1). Five volatility bins represent the range  
213 of semi-volatile organic compounds (SVOCs) ranging from  $10^{-1} \mu\text{g m}^{-3}$  to  $10^3 \mu\text{g m}^{-3}$  in  
214 saturation concentrations ( $C^*$ ). Oxidation processes are modelled by shifting  $C^*$  by a factor of  
215 10 in the next lower volatility bin, increasing the oxidation state and reducing the carbon  
216 number to account for fragmentation. OH reaction rates are assumed to be  $4 \times 10^{-11} \text{ cm}^3$   
217  $\text{molecule}^{-1} \text{ s}^{-1}$  for the reaction of semi-volatile primary vapors with OH and  $2 \times 10^{-11}$  for  
218 further aging of ASOA and POA vapours from HOA-like emissions. More details about the

VBS parameterization in CAMx can be found in Koo et al. (2014). Further aging of BSOA is not considered in this study based on previous modelling results showing over-prediction of OA when such process is taken into account (Lane et al., 2008; Murphy and Pandis, 2009). This implies that also further aging of POA vapours from BBOA-like emissions was not considered since it is performed in the same basis set. In this work we focus on the effects of a VBS framework on the total OA fraction. Aging processes and alternative VBS implementations will be discussed together with SOA and POA components in a following paper (Ciarelli et al. in prep). Three sensitivity tests were performed with different assumptions on the volatility distributions (Table 1):

- **NOVBS:** Primary organic aerosol was assumed to be non-volatile. Biogenic (isoprene, monoterpenes and sesquiterpenes) and anthropogenic (xylene, toluene and other aromatics) volatile organic compounds (VOCs) were used as precursors for secondary organic aerosol. Partitioning of condensable gases to secondary organic aerosol was calculated using a semi-volatile equilibrium approach (Strader, 1999).
- **VBS\_ROB:** Primary organic aerosol was assumed to be volatile and undergo chemical oxidation. The volatility distribution estimated by Robinson et al. (2007) was applied to HOA-like and BBOA-like emissions. Emissions of intermediate volatility organic compounds (IVOCs) were assumed to be 1.5 times those of primary organic aerosol (POA) as suggested by Robinson et al. (2007).
- **VBS\_BC:** Primary organic aerosol was assumed to be volatile and undergo chemical oxidation using the approach of Shrivastava et al. (2011) and Tsimpidi et al. (2010). The total primary emissions are roughly 3 times higher than in **VBS\_ROB**. Different volatility distributions were applied for HOA and BBOA-like emissions. IVOCs were assumed to be 1.5 times the amount of POA. This implies that for this scenario the SVOC + IVOC mass added is equal to 7.5 times the initial amount of POA. This represents the base case scenario used to evaluate gas phase and PM<sub>2.5</sub> model performance.

Based on the **VBS\_BC** base case scenario, two other sensitivity tests were performed with respect to emissions:

- **VBS\_BC\_2xBVOC:** Increased BVOCs emissions by a factor of 2.
- **VBS\_BC\_2xBBOA:** Increased BBOA-like emissions by a factor of 2.



## 2.3 Statistical methods

Statistical procedures as available in the Atmospheric Model Evaluation Tool (AMET, Apple et al., 2010) were used in this study to evaluate model performance. Daily ambient measurements of main gas phase species i.e. O<sub>3</sub>, NO<sub>2</sub>, CO, SO<sub>2</sub> and fine particulate matter (PM<sub>2.5</sub>) were extracted from the Airbase database in Europe and statistics reported in terms of mean bias (MB), mean error (ME), mean fractional bias (MFB) mean fractional error (MFE) and correlation coefficient (r).

Due to the coarse grid resolution, only rural-background stations, defined as stations far from city sources of air pollution with pollution levels determined by the integrated contribution from all sources upwind of the station (ETC/ACC, 2004/7), with at least 80% daily average observations available were considered for the statistical analysis. For PM<sub>2.5</sub> this resulted in 48 stations available for June 2006, 56 for January-February 2007, 90 for September-October 2008 and 110 stations for February-March 2009. PM<sub>2.5</sub> components were further evaluated for the February-March 2009 period where comprehensive high resolution AMS measurements at 11 European sites were available, i.e., at Barcelona, Cabauw, Chilbolton, Helsinki, Hyytiälä, Mace Head, Melpitz, Montseny, Payerne, Puy de Dôme and Vavihill (Crippa et al., 2014).

## 3 Results and discussions

### 3.1 Model evaluation

Model performance metrics for gas phase species CO, NO<sub>2</sub>, O<sub>3</sub> and SO<sub>2</sub> as well as for PM<sub>2.5</sub> are reported in Table 2 and they refer to the base case VBS\_BC.

#### NO<sub>2</sub> and O<sub>3</sub>

NO<sub>2</sub> was found to be under-predicted for all the four periods with mean fractional bias between -54% and -28% and NO<sub>2</sub> concentrations being particularly under-predicted during June 2006. Evaluation of the EURODELTA III model inter-comparison exercise showed that all models performed similarly for NO<sub>2</sub> in terms of correlation with *r* values in the range 0.6-0.7 and the spatial correlation was much higher in the range 0.7-0.9 for all models (Bessagnet et al., 2016) with a general underestimation in the afternoon. The NO<sub>2</sub> performance could be influenced by several factors:

- Uncertainties in the emission inventories. Although NO<sub>x</sub> emission estimates in Europe are thought to have an uncertainty of about  $\pm 20\%$ , the complete data set used in the inventories has much higher uncertainty (Kuenen et al., 2014). A recent study identified a significant discrepancy between emission estimates and actual flux measurements, with the highest underestimation being a factor of two in central London mainly due to under-representation of real world road traffic emissions (Vaughan et al., 2016)
- The relatively coarse resolution of the domain which may result in too low NO<sub>x</sub> emissions or isolated local events that the model cannot resolve. We report daily average time series of NO<sub>2</sub> for the period of Feb-Mar 2009 for stations in Table 2 as well as daily average time series of NO<sub>2</sub> for stations not exceeding 5 ppb (which represents 92% of the stations in Table 2) (Figure S1). The model performance for NO<sub>2</sub> significantly improved when the 5 ppb threshold was applied to the dataset. An emission map of NO for 1 March 2009 at 6 AM is reported in Figure S2. High emissions of NO are predicted in the Benelux area, Po Valley, Germany and in some of the eastern European countries. High NO emissions due to ship traffic are also visible especially in the Mediterranean Sea
- Possible positive artefacts in the chemiluminescence methods for measuring NO<sub>2</sub> may also occur when NO<sub>2</sub> is catalytically converted to NO on the molybdenum surface leading to an over-prediction of measured NO<sub>2</sub> concentrations (Steinbacher et al., 2007; Villena et al., 2012)
- Moreover, an evaluation of planetary boundary layer height (PBLH) within the EDIII shows that although the PBLH was quite well represented in general in the ECMWF IFS meteorological fields, CAMx tends to under-estimate the night-time minima and to over-estimate some daytime peaks, over-predicting the dilution of day time NO<sub>2</sub> concentrations, whereas the wind speed was relatively well reproduced (Bessagnet et al., 2016).

O<sub>3</sub> concentrations were found to be over-predicted for all the four periods with a mean fractional bias ranging from 2% to 48%. Especially in June 2006, when the photochemical activity is higher, the general under-prediction of NO<sub>x</sub> in the whole domain reduces the O<sub>3</sub> titration potential during night time.

Model performance for O<sub>3</sub> is also strongly influenced by long-range transport especially during the winter periods when the local chemical production of O<sub>3</sub> is limited. Figure S3 shows the model performance at the Mace Head station located on the west coast of Ireland for all the four periods. Especially in January-February 2007 O<sub>3</sub> concentrations were found to be over-predicted by about 10 to 20 ppb indicating that boundary conditions for O<sub>3</sub> were probably not well represented. In June 2006 and September-October 2008 O<sub>3</sub> was relatively well captured at Mace Head suggesting that the observed positive bias in O<sub>3</sub> concentrations might arise from insufficient NO<sub>x</sub> emissions to undergo titration during night time as well as not correctly represented planetary boundary layer dynamics. In February-March 2009 the model tends to under-predict the O<sub>3</sub> concentration at Mace Head and overall the O<sub>3</sub> model performance shows the lowest bias (2%). Eventually, the under-prediction of O<sub>3</sub> in the boundary condition may counteract the already mentioned deficiencies related to insufficient NO<sub>x</sub> emissions.

## **SO<sub>2</sub> and CO**

SO<sub>2</sub> concentrations were found to be slightly over-predicted for all the four periods with a mean fractional bias ranging from 14% to 36% for SO<sub>2</sub>. The daily variations of modelled and measured SO<sub>2</sub> concentrations for February-March 2009 are reported as well in Figure S1 (lower-panel) for the stations in Table 2. In general, the daily variations of modelled and measured SO<sub>2</sub> concentrations agree relatively well with each other throughout the period.

Most of the SO<sub>2</sub> emissions arise from high stack point sources which have injection heights of a few hundred meters. It might be that the vertical distribution of SO<sub>2</sub> might affect the model performance in particular near the harbors and coastal areas where ship emissions were allocated in the second layer of the model domain (extending from ~20 to 50 m above ground level) whereas they can reach up to 58 meters in deep draft vessels (SCG, 2004) and also undergo plume rise. Insufficient conversion to sulfate or too low deposition processes might also positively bias the model performance for SO<sub>2</sub>.

CO was slightly under-predicted for all periods (mean fractional bias between -11% and -31%), with highest values during the September-October 2008 period (-31%). The late summer-fall period is known to be influenced by agricultural open field burning activities which might be missing from standard emission inventories.

In general, for both SO<sub>2</sub> and CO, the model showed lower correlation coefficients with respect to other gas-phase species (*r* values from 0.20 and 0.37 for CO and from 0.37 to 0.52 for SO<sub>2</sub>).

### **PM<sub>2.5</sub>**

Of all investigated variables, CAMx shows the best statistical performance for PM<sub>2.5</sub>. For all four periods the acceptable model performance criteria recommended by Boylan and Russell (2006) for aerosols were met ( $MFE \leq +75\%$  and  $-60\% < MFB < +60\%$ ). The fractional bias ranges from less than 1% in September-October 2008 up to -13% in February-March 2009. Also the recommended model performance goals ( $MFE \leq +50\%$  and  $-30\% < MFB < +30\%$ ) were met for all periods except for January 2007. Modelled average PM<sub>2.5</sub> concentrations are shown in Fig. 1. A different spatial distribution is seen for summer and winter. In June 2006 the model predicts higher concentrations in the southern part of the domain especially over the Mediterranean Sea and North Africa (up to 35 µg m<sup>-3</sup>). On the other hand, the highest concentrations were predicted in the Po valley area (above 40 µg m<sup>-3</sup>) and in the southern part of Poland during January-February 2007. During the two colder periods (2007 and 2009) elevated concentrations of around 15 µg m<sup>-3</sup> are also visible close to urban areas such as Paris and Moscow. Figure 2 shows PM<sub>2.5</sub> variations at Airbase rural-background sites in terms of medians, 25<sup>th</sup> and 75<sup>th</sup> percentiles. In all the four periods CAMx is able to reproduce the observed monthly variation very well with some over-prediction occurring mainly from the 14<sup>th</sup> to the 17<sup>th</sup> of January 2007 and towards the end of 2008 period.

### **3.2 Detailed evaluation of PM<sub>2.5</sub> components in February-March 2009**

The modelled concentrations of non-refractory PM<sub>2.5</sub> components were compared against aerosol mass spectrometer measurements at eleven European sites for the February-March 2009 period (Crippa et al., 2014). Even though the AMS measures particles with a diameter *D* < 1 µm, the difference between the non-refractory PM<sub>1</sub> and total PM<sub>2.5</sub> mass is in general rather small as shown in Aksoyoglu et al. (2011), at least for situations without exceedingly high air pollution and situations when sea salt makes large relative contribution to PM<sub>2.5</sub>. The modelled average total non-refractory PM<sub>2.5</sub> (sum of nitrate, sulfate, ammonium and OA) concentrations match the measurements quite well with a few exceptions (Fig. 3 and Table 3). The model is able to reproduce both high concentrations observed at the urban site Barcelona and low ones at remote sites like Hyytiälä, Finland. Concentrations of inorganic aerosols are

over-predicted and OA are under-predicted at most of the stations (with similar behavior during the other investigated periods, Figure S4 and Figure S5). Very similar results were also presented by other recent studies (Knote et al., 2011). The effect of different schemes to treat OA is discussed in Sect. 3.3. At the Cabauw site nitrate was the most dominant species (Mensah et al., 2012). Especially at this site the model strongly over-predicts in particular the nitrate ( $\text{NO}_3^-$ ) fraction (by a factor of 3). A sensitivity test with 50% reduction in ammonia emissions significantly improved the modelled  $\text{NO}_3^-$  concentrations at almost all sites (Table S2) suggesting potential uncertainties in  $\text{NH}_3$  emissions and their seasonal variability. Other potential reasons for the over-prediction of  $\text{NO}_3^-$  could be related to uncertainties in removal process of  $\text{HNO}_3$  as well as dry deposition velocity of  $\text{NH}_3$ . Substantial over-predictions were found at the higher altitude site of Montseny and Puy de Dôme when compared with first model layer concentrations (ca. 200 and 800 meters a.s.l. respectively at these sites). These sites located at about 720 and 1465 meters a.s.l., are sometimes not within the PBLH during winter periods. At the Montseny site, the relatively coarse resolution of the model could also influence model performance since the site is located in a complex area about 50 km north-east of Barcelona (Pandolfi et al., 2014). Sulfate concentrations ( $\text{SO}_4^{2-}$ ) were over-predicted at almost all sites and especially at Mace Head suggesting that long-range transport of  $\text{SO}_4^{2-}$  might be positively biased.

Modelled and observed hourly concentrations of  $\text{NO}_3^-$ ,  $\text{SO}_4^{2-}$ , ammonium ( $\text{NH}_4^+$ ) and OA at Payerne are reported in Fig. 4 for March 2009 together with meteorological parameters in Fig. S6. The model was able to reproduce the meteorological parameters very well for most of the time. The temperature was slightly under-predicted at both night and day-times (with a maximum of -2 °C) whereas both the monthly variation and the absolute values of wind speed and specific humidity were reproduced well with a few under-predictions of high wind-speed (6<sup>th</sup> and 11<sup>th</sup> of March and towards the end of the simulation). The model was able to capture the three  $\text{NO}_3^-$  and  $\text{NH}_4^+$  peaks observed around the 7<sup>th</sup>, 18<sup>th</sup> and 23<sup>rd</sup> of March with a general slight over-prediction throughout the whole period. Indeed, the under-prediction in temperature during day and night time could partially explain the over-prediction of the  $\text{NO}_3^-$  fraction with more  $\text{NO}_3^-$  partitioning to the aerosol phase which also apply to the other stations used in this study. An evaluation of modelled temperature at the European scale for the February-March 2009 period confirmed that the model systematically under-predicted the 2 meter surface temperature (Bessagnet et al., 2014). All the inorganic components were over-predicted during the first four days of March 2009 with a peak around the 3<sup>rd</sup> of March,

indicating that the PBLH was probably not correctly reproduced by the model during this period. Although the temporal variation was captured, concentrations of OA were under-predicted throughout all the simulation ( $4.1 \mu\text{g m}^{-3}$  and  $1.8 \mu\text{g m}^{-3}$  observed and modelled average concentrations). Analysis of the OA fraction is discussed in the next section.

### 3.3 Organic aerosols

#### 3.3.1 Sensitivity of OA to the VBS scheme

In this section, effects of different parameterizations of the organic aerosol module on the modelled OA concentrations are discussed. The scatter plots in Fig. 5 show a comparison of daily average OA concentrations against the same AMS measurements as in Table 3 during February-March 2009. Statistics for each scenario are reported in Table 4. When the semi-volatile dynamics of primary organic aerosol is not taken into account (scenario NOVBS), the model under-predicts OA concentrations (MFB: -66%) with an observed and modelled average concentrations of  $3.0 \mu\text{g m}^{-3}$  and  $1.2 \mu\text{g m}^{-3}$  respectively. In the VBS\_ROB scenario POA emissions are allowed to evaporate following the volatility distribution proposed by Robinson et al. (2007) and to undergo chemical oxidation. In this case modelled OA concentrations decrease by about 43% with respect to NOVBS, predicting an average OA concentration of  $0.7 \mu\text{g m}^{-3}$ . On the other hand, the VBS\_BC scenario improves the OA model performance increasing the OA concentrations by about 47% with respect to NOVBS. Predicted OA concentrations are found to be  $1.7 \mu\text{g m}^{-3}$  on average (MFB: -47%). Similar behavior during winter periods was also shown in recent studies where the same VBS scheme was applied in the U.S. domain (Koo et al., 2014). Figure 6 shows the modelled total OA concentration over Europe using NOVBS, VBS\_ROB and VBS\_BC scenarios. The model predicts high OA values in the Eastern part of the domain as well as over Portugal, France and the Po Valley (VBS\_BC). Some hot-spots around large urban areas are also visible, i.e., Paris and Moscow. Higher OA concentrations in the southern part of the domain are observed in the VBS\_BC case, likely because of higher temperature and more OH radicals available in that part of the domain leading to an increase in the total organic mass upon reaction with organic vapours. This is in line with the results of Fountoukis et al. (2014) for the February-March 2009 period even though their study predicts lower concentration over the Po valley. Even though model input data and parameterizations are not the same, the VBS\_BC case in particular, uses a very similar volatility distribution as in Fountoukis et al. (2014). Our study

predicts relatively lower OA concentrations (MFB: -0.47, MFE: 0.79) compared to those reported by Fountoukis et al. (2014) (MFB: 0.02, MFE: 0.68) for February-March 2009. Unlike Fountoukis et al. (2014) our study does not include fire emissions and marine organic aerosol which may partially explain the differences. Figure 7 shows hourly modelled and observed OA concentration at Payerne for March 2009 and June 2006. In March 2009 VBS\_ROB results are lower than those in NOVBS whereas OA concentrations in VBS\_BC case are higher (see Supplementary Fig. S8 and Table S3 for average concentrations and statistics). In June 2006, the OA mass in VBS\_ROB is lower than those in NOVBS while VBS\_BC predicts similar concentrations as the NOVBS scenario ( $2.4 \mu\text{g m}^{-3}$  and  $2.6 \mu\text{g m}^{-3}$ , respectively, Fig. S9 and Table S4). It has to be noted that the NOVBS scenario predicts slightly lower OA concentration for June 2006 in Payerne with respect to our previous application (Aksoyoglu et al., 2011), mainly because of a different biogenic model being used which yields lower monoterpene and sesquiterpene emissions. Since both BVOCs and BBOA-like emissions are highly uncertain, sensitivity tests with increased biogenic and anthropogenic emissions were performed and results discussed in the next section (3.3.2).

### 3.3.2 Sensitivity of OA to BBOA-like and BVOC emissions

Emissions of BVOCs compounds (i.e. monoterpenes, isoprene and sesquiterpenes) were doubled in scenario VBS\_BC\_2xBVOC, whilst primary organic aerosol emissions from SNAP2 and SNAP10 (BBOA-like) were doubled in scenarios VBS\_BC\_2xBBOA, with other emissions and processes represented as in VBS\_BC. Figure 8 shows modelled and observed OA daily average concentrations for the VBS\_BC, VBS\_BC\_2xBVOC and VBS\_BC\_2xBBOA scenarios across the sites. Statistics for each scenario are reported in Table 5. Increasing biogenic emissions by a factor of two during February-March 2009 resulted in almost no change in the predicted total OA ( $1.7 \mu\text{g m}^{-3}$  and  $1.8 \mu\text{g m}^{-3}$  for the VBS\_BC and VBS\_BC\_2xBVOC scenarios, respectively). On the other hand, doubling the BBOA-like emissions (VBS\_BC\_2xBBOA) during the same period strongly increased the predicted OA mass (up to  $2.8 \mu\text{g m}^{-3}$  on average). As a result the mean fractional bias decreased further, from -47% to -12% averaged across the sites. This could eventually confirm other studies where substantial under-predictions in residential wood burning emissions were underlined (e.g., Bergström et al., 2012). A few points above the 2:1 lines in VBS\_BC\_2xBBOA mainly belong to the sites of Montseny, Puy de Dôme and Helsinki.

During winter periods, it is likely that elevated stations such Montseny and Puy de Dôme are most of the time above the PBLH, as suggested by previous studies for Puy de Dôme (Freney et al., 2011), whereas model concentrations are extracted from the first layer of the model. In Helsinki, BBOA emissions seem to be overestimated or the dispersion underestimated in the model.

Comparison with a warmer period in June 2006 is reported as well for Payerne where AMS measurements were also available (Fig.9). In February-March 2009 increasing BBOA-like emissions (VBS\_BC\_2xBBOA) reduced the fractional bias from -85% in VBS\_BC to -37% (Table S3) with an over-prediction occurring during 1-5 of March (Fig. 9, upper panel). As already discussed in Section 3.2, it is likely that the vertical mixing processes were not correctly represented by the model since also the inorganic components were over-predicted for the same period. Almost no change in the predicted OA mass was found when biogenic emissions were doubled (scenario VBS\_BC\_2xBVOC) (Fig. 9, upper panel) due to lower BVOCs emission during winter periods. Increasing BVOCs emissions in June 2006 increased the predicted OA mass at Payerne site especially during the 12-16 June and towards the end of the simulation period, where higher concentrations and temperature (Fig. S7) were also observed (Fig. 9, lower panel). In contrast, similar OA concentrations were predicted in Payerne for VBS\_BC and VBS\_BC\_2xBBOA during June 2006 (with averages of  $2.4 \mu\text{g m}^{-3}$  and  $2.8 \mu\text{g m}^{-3}$  respectively). This is in line with a very recent source apportionment study based on ACSM (aerosol chemical speciation monitor) measurements performed in Zürich for 13 months (February 2011 - February 2012) which revealed substantial differences between the winter (February-March) and summer (June-August)  $f_{44} / f_{43}$  space (organic mass fraction measured at mass to charge ratio 44 and 43) indicating that summer OOA (oxygenated organic aerosol) is strongly influenced by biogenic emission and winter OOA by biomass burning emission (Canonaco et al., 2015). Increased OA concentrations at Payerne in June 2006 with increased biogenic emissions were also found in other modelling studies. Bergström et al. (2012) used the VBS framework with different assumptions regarding aging processes and compared the model results for June 2006 with the AMS results at Payerne. In their study the total OA was found to be under-predicted with lower bias observed when aging processes were taken into account and biogenic emissions were increased by a factor of 3. Even though their model differs from ours in various aspects (number of volatility bins, aging processes parameterization and input data) in two of their scenario without aging of biogenic SOA Bergström et al. (2012) predicted an average OA concentration ranging from



2.6  $\mu\text{g m}^{-3}$  to 3.4  $\mu\text{g m}^{-3}$  which is similar to our base case VBS\_BC and VBS\_BC\_2xBVOC scenario (2.4  $\mu\text{g m}^{-3}$  and 3.4  $\mu\text{g m}^{-3}$ , respectively, Table S4).

### 3.3.3 OA components in summer and winter

Comparisons of the primary and secondary organic fraction at the rural site of Payerne during summer (June 2006) and winter (February-March 2009) periods are reported in Figure 10. During the winter period the VBS scheme better reproduced the primary and secondary organic aerosol components compared to the NOVBS case. In particular, For the VBS\_ROB base case, total OA concentrations were lower compared to the NOVBS case, consistent with the study of Woody et al. (2016) where the same VBS scheme was applied to the US domain. The total OA concentrations in the base case (VBS\_BC) and in the scenario with increased biomass burning emissions (VBS\_BC\_2xBBOA) were higher compared to NOVBS case, even though SOA and POA fractions were not correctly reproduced. Higher contribution from the primary fraction during winter periods was also predicted by the study of Koo et al., 2014 which deployed the same VBS scheme. Eventually, this might indicate that biomass burning precursors might be missing in this study, or that the oxidation pathways of primary organic material need to be improved in the model (up to 86% of the reacted primary organic material is still allocated in the primary set as oxidation proceeds, directly increasing the POA fraction).

Different behavior was observed for the summer period where the larger contribution of SOA to the total OA retrieved from measurements is also reproduced by the model, even though the total OA concentration was still underestimated. These results for summer are also in line with the study of Koo et al. (2014) for summer periods in the US domain using the same VBS scheme.

## 4 Conclusions

A modelling study using the regional air quality model CAMx with VBS (Volatility Basis Set) scheme was performed for the first time in Europe within the EURODELTA-III model intercomparison exercise. An evaluation for the main gas phase species and PM<sub>2.5</sub> for four different periods was performed using the European air quality database Airbase as well as AMS (Aerosol Mass Spectrometer) measurements. The period in February-March 2009 was further analyzed in more detail using different assumptions regarding the volatility of emitted

organic aerosol and emissions of precursor. The main findings of this study are summarized below:

- Although total  $\text{PM}_{2.5}$  mass concentrations and its variations were well reproduced by the model in all four periods, comparisons with AMS measurements for the February–March 2009 period revealed that the good agreement between model and measurements was most of the time due to overestimation of the inorganic fraction, especially  $\text{NO}_3^-$ , and underestimation of OA. Sensitivity tests with reduced  $\text{NH}_3$  emissions generally reduced the positive bias in  $\text{NO}_3^-$  suggesting potential uncertainties in  $\text{NH}_3$  emissions and their seasonal variability.
- In general, for all the four periods, the model under-predicted  $\text{NO}_2$  and CO concentrations. On the other hand,  $\text{O}_3$  was found to be over-predicted likely because of insufficient  $\text{NO}_x$  to undergo titration during night-time chemistry or not well captured vertical mixing processes and concentrations at the boundaries.  $\text{SO}_2$  was over-predicted presumably mainly because of uncertainties in high stack point sources representation in the model or too low deposition processes.
- Including evaporation and oxidation processes of primary organic particles with the volatility distribution proposed by Robinson et al. (2007) lowered the modelled OA mass both in winter and summer periods. On the other hand, the adjustment of the scheme by Robinson et al. (2007) suggested by Shrivastava et al. (2011) and Tsimpidi et al. (2010) brings model and observations into better agreement by reducing the negative bias for OA by about 29% (MFB) in winter.
- Sensitivity tests with increased BVOCs and BBOA-like emissions suggested that emissions from residential heating represent an important contributor to total OA during winter periods (February–March 2009). The model under-predicted the winter OA concentrations (MFB -47% for base case VBS\_BC) more than gas phase pollutants e.g.  $\text{NO}_2$  (Table 2). Eventually, increasing BBOA-like emissions by a factor of 2 brought model and observation to a reasonably good agreement even though the model still under-predicts the OA fraction (-12% MFB). This underlines the necessity to better constrain emission inventories with a focus on residential heating. Also the implementation of the VBS scheme for domestic wood burning, which substantially influences both the primary and secondary organic aerosol, should be evaluated.

- A summer period was simulated as well and results were compared at Payerne. In June 2006, the current VBS implementation could not explain the discrepancy between modelled and observed OA. During this period the difference between the model and measurements is likely to be related to BVOCs emissions which are uncertain and difficult to constrain with measurements. In this case the model was sensitive to an increase in biogenic emissions especially during periods with higher temperature and OA concentrations. The latter could confirm the importance of BVOC precursors in summer in Payerne and the way to correctly represent their evolution in the atmosphere.

## **Acknowledgements**

We thank the EURODELTA-III modelling community, especially INERIS for providing various model input data. We are grateful to ENVIRON for providing the CAMx-VBS code before its public release. Calculations of land use data were performed with the Swiss National Supercomputing Centre (CSCS). Ammonia measurements were provided kindly by FUB. We thank D. Oderbolz for developing the CAMxRunner framework to ensure reproducibility and data quality among the simulations and sensitivity tests. We thank M. Tinguely for the visualization software. We also thank G. Pirovano for helping with the pre-processing of Airbase data. This study was financially supported by the Swiss Federal Office of Environment (FOEN). JLJ was supported by NSF AGS-1360834 and EPA STAR 83587701-0. We thank D.A. Day for analysis on the DAURE dataset. Erik Swietlicki for the Vavihill dataset, A. Kiendler-Scharr for Cabauw AMS data, Evelyn Frenay for the Puy de Dôme dataset.

## References

- Aksoyoglu, S., Keller, J., Barmpadimos, I., Oderbolz, D., Lanz, V. A., Prévôt, A. S. H., and Baltensperger, U.: Aerosol modelling in ^ Europe with a focus on Switzerland during summer and winter episodes, *Atmos. Chem. Phys.*, 11, 7355–7373, doi:10.5194/acp- 11-7355-2011, 2011.
- Athanasopoulou, E., Vogel, H., Vogel, B., Tsimpidi, A. P., Pandis, S. N., Knote, C., and Fountoukis, C.: Modeling the meteorological and chemical effects of secondary organic aerosols during an EUCAARI campaign, *Atmos. Chem. Phys.*, 13, 625-645, doi:10.5194/acp-13-625-2013, 2013.
- Appel, K.W., Gilliam, R.C., Davis, N., Zubrow, A., and Howard, S.C.: Overview of the Atmospheric Model Evaluation Tool (AMET) v1.1 for evaluating meteorological and air quality models, *Environ. Modell. Softw.*, 26, 4, 434-443, 2011.
- Benedetti, A., Morcrette, J.-J., Boucher, O., Dethof, A., Engelen, R.J., Fisher, M., Flentje, H., Huneeus, N., Jones, L., Kaiser, J.W., Kinne, S., Mangold, A., Razinger, M., Simmons, A.J., Suttie, M.: Aerosol analysis and forecast in the European Centre for Medium-Range Weather Forecasts Integrated Forecast System: 2. data assimilation. *J. Geophys. Res.* 114, D13205, 2009.
- Bergström, R., Denier van der Gon, H. A. C., Prévôt, A. S. H., Yttri, K. E., and Simpson, D.: Modelling of organic aerosols over Europe (2002–2007) using a volatility basis set (VBS) framework: application of different assumptions regarding the formation of secondary organic aerosol, *Atmos. Chem. Phys.*, 12, 8499–8527, doi:10.5194/acp-12-8499-2012, 2012.
- Bessagnet, B., Colette, A., Meleux, F., Rouïl, L., Ung, A., Favez, O., Cuvelier, C., Thunis, P., Tsyro, S., Stern, R., Manders, A., Kranenburg, R., Aulinger, A., Bieser, J., Mircea, M., Briganti, G., Cappelletti, A., Calori, G., Finardi, S., Silibello, C., Ciarelli, G., Aksoyoglu, S.,

Prévôt, A., Pay, M.-T., Baldasano, J. M., García Vivanco, M., Garrido, J. L., Palomino, I.,  
Martín, F., Pirovano, G., Roberts, P., Gonzalez, L., White, L., Menut, L., Dupont, J.C.,  
Carnevale, C., and Pederzoli, A.: The EURODELTA III exercise “Model evaluation with  
observations issued from the 2009 EMEP intensive period and standard measurements in  
Feb/Mar 2009”, MSC-W Technical Report, 2014.

Bessagnet, B., Pirovano, G., Mircea, M., Cuvelier, C., Aulinger, A., Calori, G., Ciarelli, G.,  
Manders, A., Stern, R., Tsyro, S., García Vivanco, M., Thunis, P., Pay, M.-T., Colette, A.,  
Couvidat, F., Meleux, F., Rouïl, L., Ung, A., Aksoyoglu, S., Baldasano, J. M., Bieser, J.,  
Briganti, G., Cappelletti, A., D'Isodoro, M., Finardi, S., Kranenburg, R., Silibello, C.,  
Carnevale, C., Aas, W., Dupont, J.-C., Fagerli, H., Gonzalez, L., Menut, L., Prévôt, A. S. H.,  
Roberts, P., and White, L.: Presentation of the EURODELTA III inter-comparison exercise –  
Evaluation of the chemistry transport models performance on criteria pollutants and joint  
analysis with meteorology, *Atmos. Chem. Phys. Discuss.*, doi:10.5194/acp-2015-736, 2016.

Boylan, J. W. and Russell, A. G.: PM and light extinction model performance metrics, goals,  
and criteria for three-dimensional air quality models, *Atmos. Environ.*, 40, 4946–4959, 2006.

Canonaco, F., Slowik, J. G., Baltensperger, U., and Prévôt, A. S. H.: Seasonal differences in  
oxygenated organic aerosol composition: implications for emissions sources and factor  
analysis, *Atmos. Chem. Phys.*, 15, 6993-7002, doi:10.5194/acp-15-6993-2015, 2015.

Cappa, C. D. and Jimenez, J. L.: Quantitative estimates of the volatility of ambient organic  
aerosol, *Atmos. Chem. Phys.*, 10, 5409-5424, doi:10.5194/acp-10-5409-2010, 2010.

Chang, J. S., Brost, R. A., Isaksen, I. S. A., Madronich, S., Middleton, P., Stockwell, W. R.,  
and Walcek, C. J.: A three-dimensional eulerian acid deposition model : Physical concepts  
and formulation, *J. Geophys. Res.*, 92, 14681–14700, 1987.

647 Crippa, M., Canonaco, F., Lanz, V. A., Äijälä, M., Allan, J. D., Carbone, S., Capes, G.,  
648 Ceburnis, D., Dall'Osto, M., Day, D. A., DeCarlo, P. F., Ehn, M., Eriksson, A., Freney, E.,  
649 Hildebrandt Ruiz, L., Hillamo, R., Jimenez, J. L., Junninen, H., Kiendler-Scharr, A.,  
650 Kortelainen, A.-M., Kulmala, M., Laaksonen, A., Mensah, A. A., Mohr, C., Nemitz, E.,  
651 O'Dowd, C., Ovadnevaite, J., Pandis, S. N., Petäjä, T., Poulain, L., Saarikoski, S., Sellegri,  
652 K., Swietlicki, E., Tiitta, P., Worsnop, D. R., Baltensperger, U., and Prévôt, A. S. H.: Organic  
653 aerosol components derived from 25 AMS data sets across Europe using a consistent ME-2  
654 based source apportionment approach, *Atmos. Chem. Phys.*, 14, 6159– 6176,  
655 doi:10.5194/acp-14-6159-2014, 2014.

656

657 Donahue, N., Robinson, A., Stanier, C., and Pandis, S.: Coupled Partitioning, Dilution, and  
658 Chemical Aging of Semivolatile Organics, *Environ. Sci. Technol.*, 40, 2635–2643, 2006.

659

660 Donahue, N. M., Epstein, S. A., Pandis, S. N., and Robinson, A. L.: A two-dimensional  
661 volatility basis set: 1. organic-aerosol mixing thermodynamics, *Atmos. Chem. Phys.*, 11,  
662 3303–3318, doi:10.5194/acp-11-3303-2011, 2011.

663

664 Donahue, N. M., Henry, K. M., Mentel, T. F., Kiendler-Scharr, A., Spindler, C., Bohn, B.,  
665 Brauers, T., Dorn, H. P., Fuchs, H., Tillmann, R., Wahner, A., Saathoff, H., Naumann, K. H.,  
666 Mohler, O., Leisner, T., Müller, L., Reinnig, M. C., Hoffmann, T., Salo, K., Hallquist, M.,  
667 Frosch, M., Bilde, M., Tritscher, T., Barmet, P., Praplan, A. P., DeCarlo, P. F., Dommen, J.,  
668 Prevot, A. S. H., and Baltensperger, U.: Aging of biogenic secondary organic aerosol via gas-  
669 phase OH radical reactions, *P. Natl. Acad. Sci.*, 109, 13503–13508,  
670 doi:10.1073/pnas.1115186109, 2012a.

671

672 Donahue, N. M., Kroll, J. H., Pandis, S. N., and Robinson, A. L.: A two-dimensional  
673 volatility basis set – Part 2: Diagnostics of organic-aerosol evolution, *Atmos. Chem. Phys.*,  
674 12, 615–634, doi:10.5194/acp-12-615-2012, 2012b.

675

ETC/ACC, Improvement of classifications European monitoring stations for AirBase - A quality control, Technical Paper 2004/7.

Environ: User's Guide, Comprehensive Air Quality Model with Extensions (CAMx), Version 5.40, Environ International Corporation, California, 2011.

Freney, E. J., Sellegri, K., Canonaco, F., Boulon, J., Hervo, M., Weigel, R., Pichon, J. M., Colomb, A., Prévôt, A. S. H., and Laj, P.: Seasonal variations in aerosol particle composition at the puy-de-Dôme research station in France, *Atmos. Chem. Phys.*, 11, 13047-13059, doi:10.5194/acp-11-13047-2011, 2011.

Fountoukis, C., Racherla, P. N., Denier van der Gon, H. A. C., Polymeneas, P., Charalampidis, P. E., Pilinis, C., Wiedensohler, A., Dall'Osto, M., O'Dowd, C., and Pandis, S. N.: Evaluation of a three-dimensional chemical transport model (PMCAMx) in the European domain during the EUCAARI May 2008 campaign, *Atmos. Chem. Phys.*, 11, 10331–10347, doi:10.5194/acp-11-10331-2011, 2011.

Fountoukis, C., Megaritis, A. G., Skyllakou, K., Charalampidis, P. E., Pilinis, C., Denier van der Gon, H. A. C., Crippa, M., Canonaco, F., Mohr, C., Prévôt, A. S. H., Allan, J. D., Poulain, L., Petäjä, T., Tiitta, P., Carbone, S., Kiendler-Scharr, A., Nemitz, E., O'Dowd, C., Swietlicki, E., and Pandis, S. N.: Organic aerosol concentration and composition over Europe: insights from comparison of regional model predictions with aerosol mass spectrometer factor analysis, *Atmos. Chem. Phys.*, 14, 9061-9076, doi:10.5194/acp-14-9061-2014, 2014.

Guenther, A. B., Jiang, X., Heald, C. L., Sakulyanontvittaya, T., Duhl, T., Emmons, L. K., and Wang, X.: The Model of Emissions of Gases and Aerosols from Nature version 2.1 (MEGAN2.1): an extended and updated framework for modeling biogenic emissions, *Geosci. Model Dev.*, 5, 1471–1492, doi:10.5194/gmd-5-1471-2012, 2012.

Hallquist, M., Wenger, J. C., Baltensperger, U., Rudich, Y., Simpson, D., Claeys, M., Dommen, J., Donahue, N. M., George, C., Goldstein, A. H., Hamilton, J. F., Herrmann, H.,

706 Hoffmann, T., Iinuma, Y., Jang, M., Jenkin, M. E., Jimenez, J. L., Kiendler-Scharr, A.,  
 707 Maenhaut, W., McFiggans, G., Mentel, Th. F., Monod, A., Prévôt, A. S. H., Seinfeld, J. H.,  
 708 Surratt, J. D., Szmigielski, R., and Wildt, J.: The formation, properties and impact of  
 709 secondary organic aerosol: current and emerging issues, *Atmos. Chem. Phys.*, 9, 5155–5236,  
 710 doi:10.5194/acp-9-5155- 2009, 2009.  
 711  
 712 Hodzic, A., Jimenez, J. L., Madronich, S., Canagaratna, M. R., DeCarlo, P. F., Kleinman, L.,  
 713 and Fast, J.: Modeling organic aerosols in a megacity: potential contribution of semi-volatile  
 714 and intermediate volatility primary organic compounds to secondary organic aerosol  
 715 formation, *Atmos. Chem. Phys.*, 10, 5491-5514, doi:10.5194/acp-10-5491-2010, 2010.  
 716 Inness, A., Baier, F., Benedetti, A., Bouarar, I., Chabrillat, S., Clark, H., Clerbaux, C.,  
 717 Coheur, P., Engelen, R. J., Errera, Q., Flemming, J., George, M., Granier, C., Hadji-Lazaro,  
 718 J., Huijnen, V., Hurtmans, D., Jones, L., Kaiser, J. W., Kapsomenakis, J., Lefever, K., Leitão,  
 719 J., Razinger, M., Richter, A., Schultz, M. G., Simmons, A. J., Suttie, M., Stein, O., Thépaut,  
 720 J.-N., Thouret, V., Vrekoussis, M., Zerefos, C., and the MACC team: The MACC reanalysis:  
 721 an 8 yr data set of atmospheric composition, *Atmos. Chem. Phys.*, 13, 4073-4109,  
 722 doi:10.5194/acp-13-4073-2013, 2013.  
 723  
 724 Jo, D. S., Park, R. J., Kim, M. J., and Spracklen, D. V.: Effects of chemical aging on global  
 725 secondary organic aerosol using the volatility basis set approach, *Atmos. Environ.*, 81, 230–  
 726 244, doi:10.1016/j.atmosenv.2013.08.055, 2013.  
 727  
 728 Knote, C., Brunner, D., Vogel, H., Allan, J., Asmi, A., Äijälä, M., Carbone, S., van der Gon,  
 729 H. D., Jimenez, J. L., Kiendler-Scharr, A., Mohr, C., Poulain, L., Prévôt, A. S. H., Swietlicki,  
 730 E., and Vogel, B.: Towards an online-coupled chemistry-climate model: evaluation of trace  
 731 gases and aerosols in COSMO-ART, *Geosci. Model Dev.*, 4, 1077-1102, doi:10.5194/gmd-4-  
 732 1077-2011, 2011.  
 733  
 734 Koo, B., Knipping, E., Yarwood, G.: 1.5-Dimensional volatility basis set approach for  
 735 modeling organic aerosol in CAMx and CMAQ, *Atmos Environ.*, 95: 158-164., 2014.



737 Kuenen, J. J. P., Denier van der Gon, H. A. C., Visschedijk, A., Van der Brugh, H., and Van  
 738 Gijlswijk, R.: MACC European emission inventory for the years 2003–2007, TNO report  
 739 TNO- 060-UT-2011-00588, TNO, Utrecht, 2011.

740

741 Kulmala, M., Asmi, A., Lappalainen, H. K., Carslaw, K. S., Pöschl, U., Baltensperger, U.,  
 742 Hov, Ø., Brenquier, J.-L., Pandis, S. N., Facchini, M. C., Hansson, H.-C., Wiedensohler, A.,  
 743 and O'Dowd, C. D.: Introduction: European Integrated Project on Aerosol Cloud Climate and  
 744 Air Quality interactions (EUCAARI) – integrating aerosol research from nano to global  
 745 scales, *Atmos. Chem. Phys.*, 9, 2825–2841, doi:10.5194/acp-9-2825-2009, 2009.

746 Kulmala, M., Asmi, A., Lappalainen, H. K., Baltensperger, U., Brenguier, J.-L., Facchini, M.  
 747 C., Hansson, H.-C., Hov, Ø., O'Dowd, C. D., Pöschl, U., Wiedensohler, A., Boers, R.,  
 748 Boucher, O., de Leeuw, G., Denier van der Gon, H. A. C., Feichter, J., Krejci, R., Laj, P.,  
 749 Lihavainen, H., Lohmann, U., McFiggans, G., Mentel, T., Pilinis, C., Riipinen, I., Schulz, M.,  
 750 Stohl, A., Swietlicki, E., Vignati, E., Alves, C., Amann, M., Ammann, M., Arabas, S., Artaxo,  
 751 P., Baars, H., Beddows, D. C. S., Bergström, R., Beukes, J. P., Bilde, M., Burkhardt, J. F.,  
 752 Canonaco, F., Clegg, S. L., Coe, H., Crumeyrolle, S., D'Anna, B., Decesari, S., Gilardoni, S.,  
 753 Fischer, M., Fjaeraa, A. M., Fountoukis, C., George, C., Gomes, L., Halloran, P., Hamburger,  
 754 T., Harrison, R. M., Herrmann, H., Hoffmann, T., Hoose, C., Hu, M., Hyvärinen, A., Hörrak,  
 755 U., Iinuma, Y., Iversen, T., Josipovic, M., Kanakidou, M., Kiendler-Scharr, A., Kirkevåg, A.,  
 756 Kiss, G., Klimont, Z., Kolmonen, P., Komppula, M., Kristjánsson, J.-E., Laakso, L.,  
 757 Laaksonen, A., Labonnote, L., Lanz, V. A., Lehtinen, K. E. J., Rizzo, L. V., Makkonen, R.,  
 758 Manninen, H. E., McMeeking, G., Merikanto, J., Minikin, A., Mirme, S., Morgan, W. T.,  
 759 Nemitz, E., O'Donnell, D., Panwar, T. S., Pawlowska, H., Petzold, A., Pienaar, J. J., Pio, C.,  
 760 Plass-Duelmer, C., Prévôt, A. S. H., Pryor, S., Reddington, C. L., Roberts, G., Rosenfeld, D.,  
 761 Schwarz, J., Seland, Ø., Sellegri, K., Shen, X. J., Shiraiwa, M., Siebert, H., Sierau, B.,  
 762 Simpson, D., Sun, J. Y., Topping, D., Tunved, P., Vaattovaara, P., Vakkari, V., Veefkind, J.  
 763 P., Visschedijk, A., Vuollekoski, H., Vuolo, R., Wehner, B., Wildt, J., Woodward, S.,  
 764 Worsnop, D. R., van Zadelhoff, G.-J., Zardini, A. A., Zhang, K., van Zyl, P. G., Kerminen,  
 765 V.-M., S Carslaw, K., and Pandis, S. N.: General overview: European Integrated project on  
 766 Aerosol Cloud Climate and Air Quality interactions (EUCAARI) – integrating aerosol

767 research from nano to global scales, *Atmos. Chem. Phys.*, 11, 13061–13143, doi:10.5194/acp-  
 768 11-13061-2011, 2011.

769

770 Lane, T. E., Donahue, N. M., and Pandis, S. N.: Simulating secondary organic aerosol  
 771 formation using the volatility basis-set approach in a chemical transport model, *Atmos.*  
 772 *Environ.*, 42, 7439–7451, doi:10.1016/j.atmosenv.2008.06.026, 2008.

773

774 Langmann, B., Sellegri, K., and Freney, E.: Secondary organic aerosol formation during June  
 775 2010 in Central Europe: measurements and modelling studies with a mixed thermodynamic-  
 776 kinetic approach, *Atmos. Chem. Phys.*, 14, 3831-3842, doi:10.5194/acp-14-3831-2014, 2014.

777 Li, Y. P., Elbern, H., Lu, K. D., Friese, E., Kiendler-Scharr, A., Mentel, Th. F., Wang, X. S.,  
 778 Wahner, A., and Zhang, Y. H.: Updated aerosol module and its application to simulate  
 779 secondary organic aerosols during IMPACT campaign May 2008, *Atmos. Chem. Phys.*, 13,  
 780 6289-6304, doi:10.5194/acp-13-6289-2013, 2013.

781

782 Madronich, S.: The Tropospheric Visible Ultra-violet (TUV) model web page, National  
 783 Center for Atmospheric Research, Boulder, CO., <http://www.acd.ucar.edu/TUV/>, 2002.

784

785 Mensah, A. A., Holzinger, R., Otjes, R., Trimborn, A., Mentel, Th. F., ten Brink, H., Henzing,  
 786 B., and Kiendler-Scharr, A.: Aerosol chemical composition at Cabauw, The Netherlands as  
 787 observed in two intensive periods in May 2008 and March 2009, *Atmos. Chem. Phys.*, 12,  
 788 4723-4742, doi:10.5194/acp-12-4723-2012, 2012.

789

790 Murphy, B. N. and Pandis, S. N.: Simulating the formation of semivolatile primary and  
 791 secondary organic aerosol in a regional chemical transport model, *Environ. Sci. Technol.*, 43,  
 792 4722– 4728, 2009.

793

794 Murphy, B. N., Donahue, N. M., Fountoukis, C., Dall' Osto, M., O'Dowd, C., Kiendler-  
 795 Scharr, A., and Pandis, S. N.: Functionalization and fragmentation during ambient organic

796 aerosol aging: application of the 2-D volatility basis set to field studies, *Atmos. Chem. Phys.*,  
 797 12, 10797-10816, doi:10.5194/acp-12-10797-2012, 2012.

798

799 NASA/GSFC, Total ozone mapping spectrometer: [http://toms.gsfc.](http://toms.gsfc.nasa.gov/ozone/ozone.html)  
 800 [nasa.gov/ozone/ozone.html](http://toms.gsfc.nasa.gov/ozone/ozone.html), 2005.

801

802 Nenes, A., Pandis, S. N., and Pilinis, C.: ISORROPIA: A new thermodynamic equilibrium  
 803 model for multiphase multicomponent inorganic aerosols, *Aquatic Geochemistry*, 4, 123–152,  
 804 1998.

805

806 Pandolfi, M., Querol, X., Alastuey, A., Jimenez, J.L., Jorba, O., Day, D., Ortega, A., Cubison,  
 807 M.J., Comerón, A., Sicard, M., Mohr, C., Prévôt, A.S.H., Minguillón, M.C., Pey, J.,  
 808 Baldasano, J.M., Burkhardt, J.F., Seco, R., Peñuelas, J., Van Drooge, B.L., Artiñano, B., Di  
 809 Marco, C., Nemitz, E., Schallhart, S., Metzger, A., Hansel, A., Lorente, J., Ng, S., Jayne J.,  
 810 and Szidat, S.: Effects of sources and meteorology on particulate matter in the Western  
 811 Mediterranean Basin: an overview of the DAURE campaign, *J. Geophys. Res. Atmos.*, 119  
 812 <http://dx.doi.org/10.1002/2013JD021079>, 2014.

813

814 Passant, N. R.: Speciation of UK emissions of non-methane volatile organic compounds,  
 815 AEA Technology, Culham, 289, 2002.

816

817 Robinson, A. L., Donahue, N. M., Shrivastava, M. K., Weitkamp, E. A., Sage, A. M.,  
 818 Grieshop, A. P., Lane, T. E., Pierce, J. R., and Pandis, S. N.: Rethinking Organic Aerosols:  
 819 Semivolatile Emissions and Photochemical Aging, *Science*, 315, 1259–1262,  
 820 doi:10.1126/science.1133061, 2007.

821

822 Shrivastava, M., Fast, J., Easter, R., Gustafson Jr., W. I., Zaveri, R. A., Jimenez, J. L., Saide,  
 823 P., and Hodzic, A.: Modeling organic aerosols in a megacity: comparison of simple and

824 complex representations of the volatility basis set approach, *Atmos. Chem. Phys.*, 11, 6639–  
825 6662, doi:10.5194/acp-11-6639-2011, 2011.

826

827 Solazzo, E., Bianconi, R., Pirovano, G., Matthias, V., Vautard, R., Moran, M. D., Appel, K.  
828 W., Bessagnet, B., Brandt, J., Christensen, J. H., Chemel, C., Coll, I., Ferreira, J., Forkel, R.,  
829 Francis, X. V., Grell, G., Grossi, P., Hansen, A. B., Miranda, A. I., Nopmongcol, U., Prank,  
830 M., Sartelet, K. N., Schaap, M., Silver, J. D., Sokhi, R. S., Vira, J., Werhahn, J., Wolke, R.,  
831 Yarwood, G., Zhang, J., Rao, S. T., and Galmarini, S.: Operational model evaluation for  
832 particulate matter in Europe and North America in the context of AQMEII, *Atmos. Environ.*,  
833 53, 75–92, doi:10.1016/j.atmosenv.2012.02.045, 2012a.

834

835 Starcrest Consulting Group, LLC, Starcrest Consulting Group, LLC.: Port-Wide Baseline Air  
836 Emissions Inventory. Prepared for the Port of Los Angeles, California, 2004.

837

838 Steinbacher, M., Zellweger, C., Schwarzenbach, B., Bugmann, S., Buchmann, B., Ordóñez,  
839 C., Prevot, A. S. H., and Hueglin, C.: Nitrogen Oxides Measurements at Rural Sites in  
840 Switzerland: Bias of Conventional Measurement Techniques, *J. Geophys. Res.*, 2007.

841

842 Strader, R., Lurmann, F., and Pandis, S. N.: Evaluation of secondary organic aerosol  
843 formation in winter, *Atmos. Environ.*, 33, 4849– 4863, 1999.

844

845 Tsigaridis, K., Daskalakis, N., Kanakidou, M., Adams, P. J., Artaxo, P., Bahadur, R.,  
846 Balkanski, Y., Bauer, S. E., Bellouin, N., Benedetti, A., Bergman, T., Berntsen, T. K.,  
847 Beukes, J. P., Bian, H., Carslaw, K. S., Chin, M., Curci, G., Diehl, T., Easter, R. C., Ghan, S.  
848 J., Gong, S. L., Hodzic, A., Hoyle, C. R., Iversen, T., Jathar, S., Jimenez, J. L., Kaiser, J. W.,  
849 Kirkevåg, A., Koch, D., Kokkola, H., Lee, Y. H., Lin, G., Liu, X., Luo, G., Ma, X., Mann, G.  
850 W., Mihalopoulos, N., Morcrette, J.-J., Müller, J.-F., Myhre, G., Myriokefalitakis, S., Ng, N.  
851 L., O'Donnell, D., Penner, J. E., Pozzoli, L., Pringle, K. J., Russell, L. M., Schulz, M., Sciare,  
852 J., Seland, Ø., Shindell, D. T., Sillman, S., Skeie, R. B., Spracklen, D., Stavrakou, T.,  
853 Steenrod, S. D., Takemura, T., Tiitta, P., Tilmes, S., Tost, H., van Noije, T., van Zyl, P. G.,

von Salzen, K., Yu, F., Wang, Z., Wang, Z., Zaveri, R. A., Zhang, H., Zhang, K., Zhang, Q.,  
and Zhang, X.: The AeroCom evaluation and intercomparison of organic aerosol in global  
models, *Atmos. Chem. Phys.*, 14, 10845-10895, doi:10.5194/acp-14-10845-2014, 2014.

Tsimpidi, A. P., Karydis, V. A., Zavala, M., Lei, W., Molina, L., Ulbrich, I. M., Jimenez, J.  
L., and Pandis, S. N.: Evaluation of the volatility basis-set approach for the simulation of  
organic aerosol formation in the Mexico City metropolitan area, *Atmos. Chem. Phys.*, 10,  
525-546, doi:10.5194/acp-10-525-2010, 2010.

Tørseth, K., Aas, W., Breivik, K., Fjæraa, A. M., Fiebig, M., Hjellbrekke, A. G., Lund Myhre,  
C., Solberg, S., and Yttri, K. E.: Introduction to the European Monitoring and Evaluation  
Programme (EMEP) and observed atmospheric composition change during 1972–2009,  
*Atmos. Chem. Phys.*, 12, 5447–5481, doi:10.5194/acp-12-5447-2012, 2012.

Vestreng, V., Myhre, G., Fagerli, H., Reis, S., and Tarrasón, L.: Twenty-five years of  
continuous sulphur dioxide emission reduction in Europe, *Atmos. Chem. Phys.*, 7, 3663-3681,  
doi:10.5194/acp-7-3663-2007, 2007.

Vaughan, A.R., Lee, J.D., Misztal, P.K., Metzger, S., Shaw, M.D., Lewis, A.C., Purvis, R.M.,  
Carslaw, D.C., Goldstein, A.H., Hewitt, C.N., Davison, B., Beevers, S.D., Karl, T.G.,  
Spatially resolved flux measurements of NO<sub>x</sub> from London suggest significantly higher  
emissions than predicted by inventories. *Faraday Discuss.* doi:10.1039/C5FD00170F, 2016

Villena, G., Bejan, I., Kurtenbach, R., Wiesen, P., and Kleffmann, J.: Interferences of  
commercial NO<sub>2</sub> instruments in the urban atmosphere and in a smog chamber, *Atmos. Meas.*  
*Tech.*, 5, 149-159, doi:10.5194/amt-5-149-2012, 2012.

WHO, Burden of disease from Ambient Air Pollution for 2012 - Summary of results, 2014a.

882 Yarwood, G., Rao, S., Yocke, M., and Whitten, G. Z.: Updates to the Carbon Bond Chemical  
883 Mechanism: CB05 Yocke & Company, Novato, CA 94945RT-04-00675, 2005.

884

885 Zhang, L., Brook, J. R., and Vet, R.: A revised parameterization for gaseous dry deposition in  
886 air-quality models, *Atmos. Chem. Phys.*, 3, 2067–2082, doi:10.5194/acp-3-2067-2003, 2003.

887

888 Zhang, Q. J., Beekmann, M., Drewnick, F., Freutel, F., Schneider, J., Crippa, M., Prevot, A.  
889 S. H., Baltensperger, U., Poulain, L., Wiedensohler, A., Sciare, J., Gros, V., Borbon, A.,  
890 Colomb, A., Michoud, V., Doussin, J.-F., Denier van der Gon, H. A. C., Haeffelin, M.,  
891 Dupont, J.-C., Siour, G., Petetin, H., Bessagnet, B., Pandis, S. N., Hodzic, A., Sanchez, O.,  
892 Honoré, C., and Perrussel, O.: Formation of organic aerosol in the Paris region during the  
893 MEGAPOLI summer campaign: evaluation of the volatility-basis-set approach within the  
894 CHIMERE model, *Atmos. Chem. Phys.*, 13, 5767-5790, doi:10.5194/acp-13-5767-2013,  
895 2013.

896

## 5 Figures and Tables

Table 1. Volatility distributions used for different scenarios.

Scenarios	POA emission sources	Emission fraction for volatility bin with C* of				
		0	1	10	100	1000
NOVBS (non-volatile CAMxv5.40)	HOA-like	1.00	-	-	-	-
	BBOA-like	1.00	-	-	-	-
VBS_ROB (Robinson et al., 2007 )	HOA-like	0.09	0.09	0.14	0.18	0.5
	BBOA-like	0.09	0.09	0.14	0.18	0.5
VBS_BC (Tsimpidi et al., 2010 and Shrivastava et al., 2011)	HOA-like	0.40	0.26	0.40	0.51	1.43
	BBOA-like	0.27	0.27	0.42	0.54	1.50

902 Table 2. Model gas phase and PM<sub>2.5</sub> performance for the EDIII field campaigns (base case  
 903 VBS\_BC).

Species	Number of sites	Observed mean (ppb) ( $\mu\text{g m}^{-3}$ for PM <sub>2.5</sub> )	Modelled mean (ppb) ( $\mu\text{g m}^{-3}$ for PM <sub>2.5</sub> )	MB (ppb) ( $\mu\text{g m}^{-3}$ for PM <sub>2.5</sub> )	ME (ppb) ( $\mu\text{g m}^{-3}$ for PM <sub>2.5</sub> )	MFB [-]	MFE [-]	r
June 2006								
CO	36	192.0	158.0	-34.2	80.7	-0.12	0.36	0.20
NO <sub>2</sub>	320	4.1	2.3	-1.9	2.2	-0.54	0.68	0.55
O <sub>3</sub>	460	42.3	51.2	8.9	10.8	0.21	0.24	0.57
PM <sub>2.5</sub>	48	12.0	11.7	-0.3	4.5	-0.07	0.39	0.55
SO <sub>2</sub>	263	1.0	1.2	0.2	0.7	0.14	0.67	0.52
Jan-Feb 2007								
CO	45	248.0	191.0	-57.8	107.0	-0.11	0.37	0.21
NO <sub>2</sub>	337	6.5	4.4	-2.2	3.2	-0.28	0.57	0.68
O <sub>3</sub>	455	23.5	35.8	12.3	12.6	0.48	0.49	0.61
PM <sub>2.5</sub>	56	11.7	12.8	1.0	6.1	-0.04	0.56	0.69
SO <sub>2</sub>	271	1.3	1.7	0.4	1.1	0.36	0.75	0.46
Sep-Oct 2008								
CO	53	208.0	136.0	-72.0	91.4	-0.31	0.48	0.27
NO <sub>2</sub>	370	5.3	3.7	-1.7	2.5	-0.28	0.56	0.62
O <sub>3</sub>	465	24.3	32.5	8.2	9.6	0.32	0.37	0.50
PM <sub>2.5</sub>	90	13.0	14.1	1.0	5.7	<0.01	0.46	0.76
SO <sub>2</sub>	256	0.9	1.1	0.2	0.8	0.25	0.74	0.37
Feb-Mar 2009								
CO	57	262.0	170.0	-91.6	119.0	-0.26	0.48	0.37
NO <sub>2</sub>	380	6.0	3.9	-2.0	2.8	-0.33	0.56	0.61
O <sub>3</sub>	488	32.7	33.0	0.2	7.1	0.02	0.23	0.55
PM <sub>2.5</sub>	110	15.1	13.0	-2.1	6.4	-0.13	0.50	0.71
SO <sub>2</sub>	257	1.0	1.3	0.3	0.9	0.23	0.76	0.45

904

905

906



907 Table 3. Statistical analysis of nitrate, ammonium, sulfate and organic aerosol in base case  
 908 (VBS\_BC) for February-March 2009 at different AMS sites.

909

Site	Mean observed ( $\mu\text{g}/\text{m}^3$ )	Mean modelled ( $\mu\text{g}/\text{m}^3$ )	MB $\mu\text{g m}^{-3}$	ME $\mu\text{g m}^{-3}$	MFB [-]	MFE [-]
$\text{NO}_3^-$						
Barcelona	3.6	5.8	2.19	3.98	0.35	0.98
Cabauw	2.2	6.7	4.49	4.58	0.85	1.01
Chilbolton	2.7	4.0	1.33	2.21	0.02	0.76
Helsinki	1.0	1.9	0.93	1.30	0.29	0.92
Hyytiälä	0.2	1.0	0.75	0.83	0.21	1.09
Mace Head	0.6	1.7	1.11	1.12	0.14	0.70
Melpitz	3.1	4.3	1.25	2.41	0.35	0.71
Montseny	3.1	5.9	2.83	4.31	0.38	1.00
Payerne	3.9	5.7	1.81	2.83	0.34	0.61
Puy de Dôme	0.9	2.7	1.81	2.17	1.13	1.30
Vavihill	2.8	3.7	0.89	2.17	0.14	0.78
$\text{NH}_4^+$						
Barcelona	1.6	2.5	0.92	1.41	0.42	0.71
Cabauw	1.0	2.7	1.73	1.75	0.95	0.97
Chilbolton	1.3	2.0	0.68	1.02	0.39	0.61
Helsinki	0.8	1.3	0.52	0.59	0.51	0.60
Hyytiälä	0.4	0.8	0.43	0.48	0.55	0.70
Melpitz	1.4	2.1	0.72	1.11	0.45	0.69
Montseny	1.7	2.6	0.92	1.58	0.39	0.74
Payerne	1.7	2.5	0.80	1.15	0.36	0.56
Puy de Dôme	0.7	1.2	0.51	0.87	0.83	1.07
Vavihill	1.6	1.9	0.38	0.90	0.17	0.56
$\text{SO}_4^{2-}$						
Barcelona	2.7	2.3	-0.44	1.25	-0.19	0.48
Cabauw	1.0	2.1	1.13	1.34	0.73	0.85
Chilbolton	1.3	2.2	0.91	1.33	0.45	0.70
Helsinki	2.4	2.2	-0.24	0.92	-0.04	0.43
Hyytiälä	1.4	1.7	0.26	0.73	0.09	0.58
Mace Head	0.4	1.2	0.83	0.89	1.04	1.12
Melpitz	1.1	2.2	1.15	1.40	0.54	0.76
Montseny	1.4	2.3	0.97	1.19	0.55	0.64

Payerne	1.1	2.1	1.06	1.16	0.62	0.70
Puy de Dôme	0.4	1.1	0.77	0.82	1.14	1.19
Vavihill	1.6	2.3	0.73	1.05	0.18	0.54

---

OA						
Barcelona	8.2	3.1	-5.11	5.15	-0.80	0.82
Cabauw	1.2	1.1	-0.14	0.53	-0.13	0.50
Chilbolton	2.4	0.7	-1.70	1.70	-1.09	1.10
Helsinki	2.7	2.9	0.26	1.64	0.08	0.62
Hyytiälä	1.3	1.0	-0.28	0.52	-0.48	0.60
Mace Head	0.8	0.4	-0.38	0.43	-0.29	0.70
Melpitz	1.5	0.5	-0.95	0.98	-0.94	0.97
Montseny	3.1	3.9	0.88	1.88	0.31	0.57
Payerne	4.1	1.8	-2.33	2.43	-0.85	0.90
Puy de Dôme	0.6	1.4	0.78	0.96	0.68	0.91
Vavihill	3.9	1.4	-2.53	2.53	-1.04	1.04

910

911 Table 4. Statistical analysis of OA for NOVBS, VBS\_ROB and VBS\_BC scenarios for the 11  
912 AMS sites for February-March 2009.

Scenario	Mean observed OA ( $\mu\text{g m}^{-3}$ )	Mean modelled OA ( $\mu\text{g m}^{-3}$ )	MB ( $\mu\text{g m}^{-3}$ )	ME ( $\mu\text{g m}^{-3}$ )	MFB [-]	MFE [-]
NOVBS	3.0	1.2	-1.8	2.0	-0.66	0.88
VBS_ROB	3.0	0.7	-2.3	2.4	-1.08	1.19
VBS_BC (base case)	3.0	1.7	-1.2	1.8	-0.47	0.79

913

914 Table 5. Statistical analysis of OA for VBS\_BC, VBS\_BC\_2xBVOC and VBS\_BC\_2xBBOA  
915 scenarios for the 11 AMS sites for February-March 2009.

Scenario	Mean observed OA ( $\mu\text{g m}^{-3}$ )	Mean modelled OA ( $\mu\text{g m}^{-3}$ )	MB ( $\mu\text{g m}^{-3}$ )	ME ( $\mu\text{g m}^{-3}$ )	MFB [-]	MFE [-]
VBS_BC (base case)	3.0	1.7	-1.2	1.8	-0.47	0.79
VBS_BC_2xBVOC	3.0	1.8	-1.2	1.8	-0.46	0.78
VBS_BC_2xBBOA	3.0	2.8	-0.1	1.9	-0.12	0.69

916

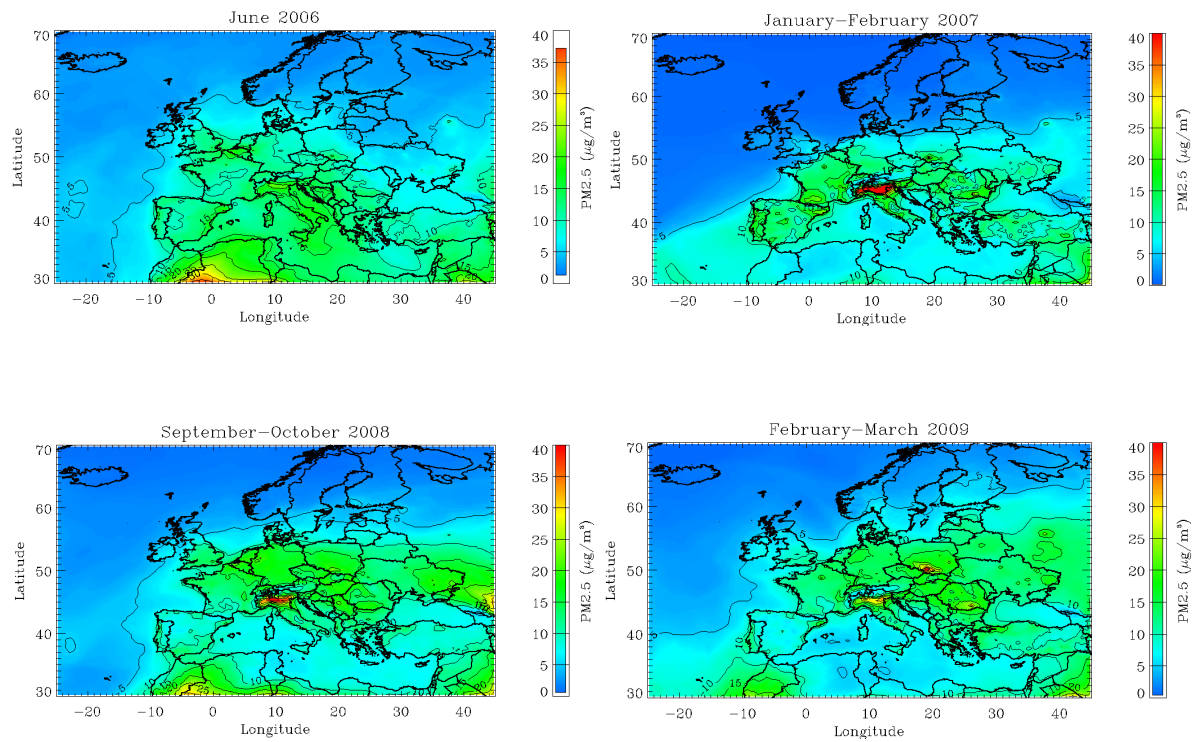
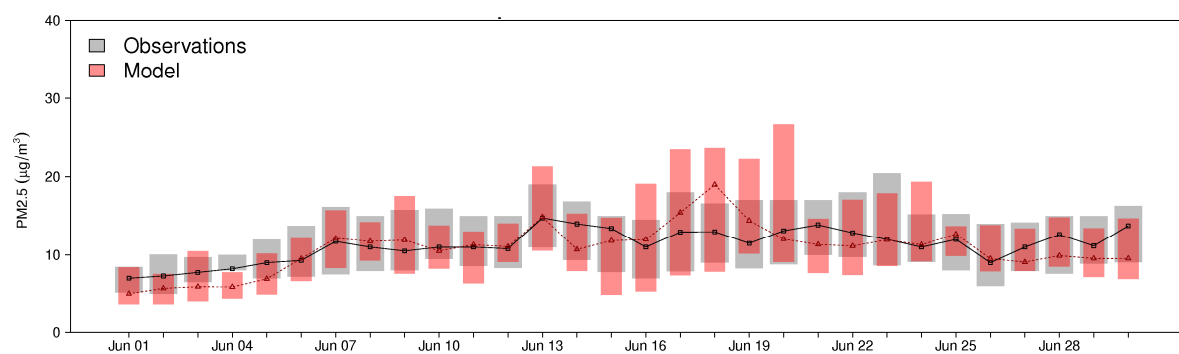
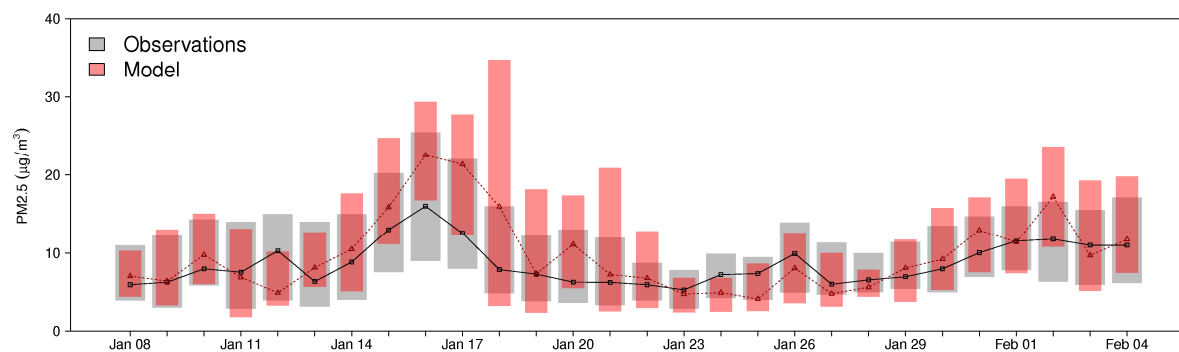


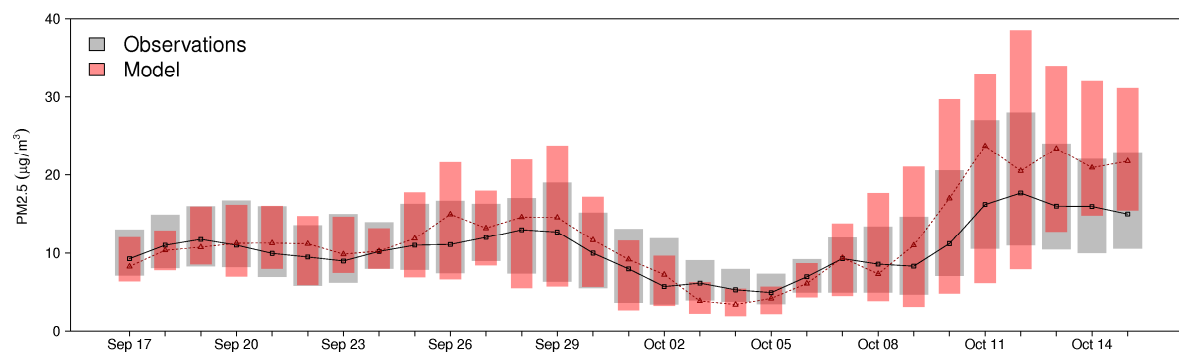
Figure 1. Modelled average PM<sub>2.5</sub> concentrations for June 2006, January-February 2007, September-October 2008 and February-March 2009 (top to bottom) based on the base case (VBS\_BC). Note that the color scale was limited to maximum of 40 µg/m<sup>3</sup> to facilitate comparison of the panels.



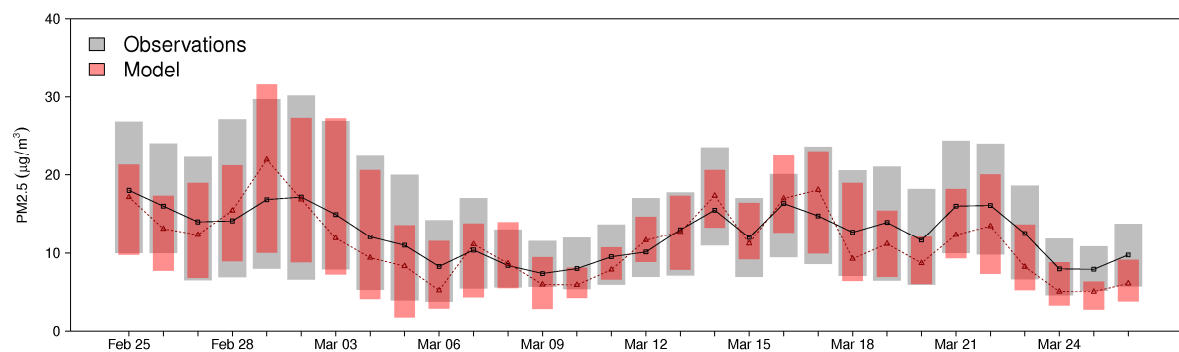
926



927



928



929

930 Figure 2. Comparison of modelled (red) and measured (grey) PM<sub>2.5</sub> concentrations at AirBase  
 931 rural background sites. The extent of the bars indicates the 25<sup>th</sup> and 75<sup>th</sup> percentile. The black

932 and red lines are observed and modelled median, respectively. The numbers of sites are 48,  
933 58, 90, and 110 from top to down. Based on base case (VBS\_BC).  
934

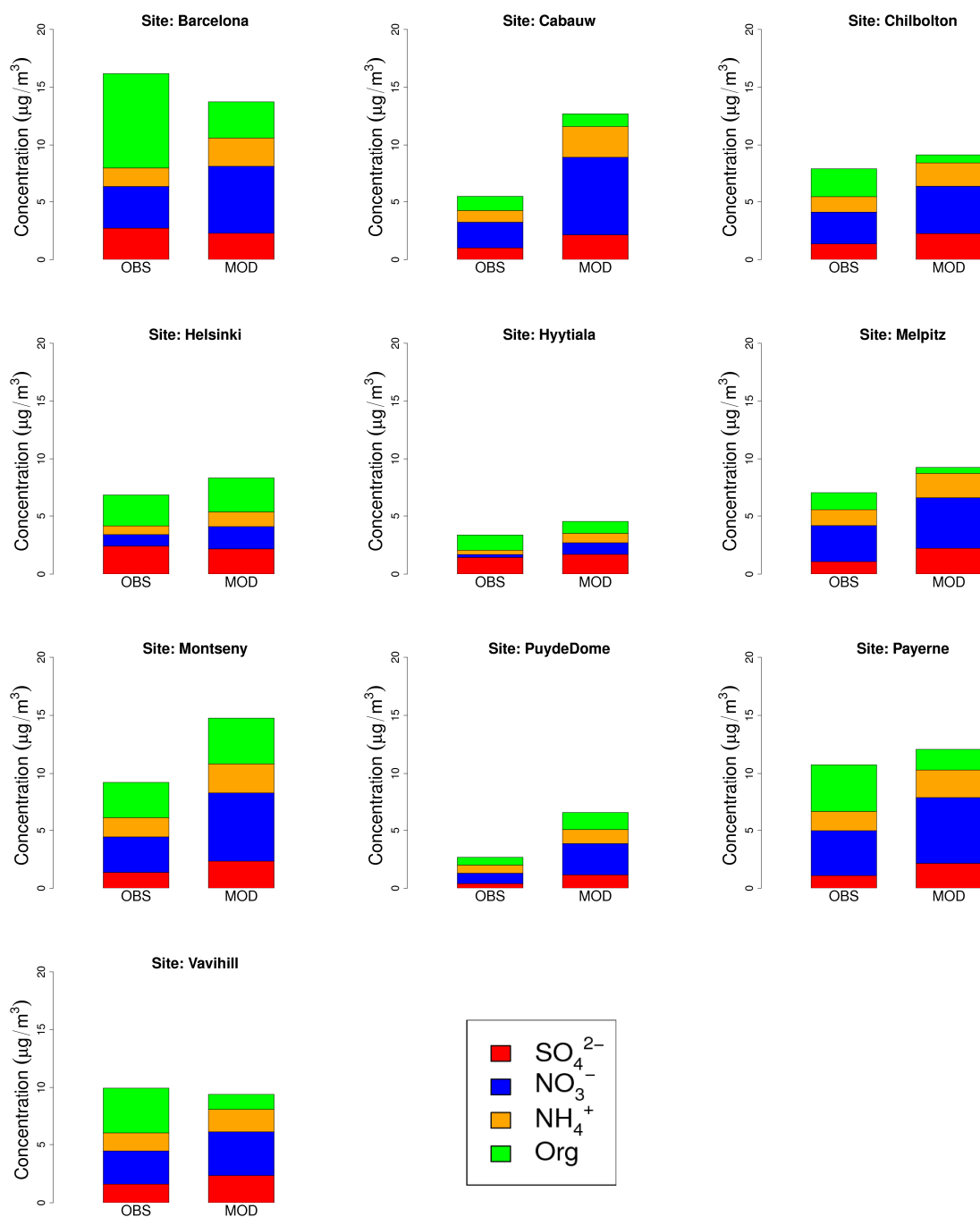


Figure 3. Comparison of observed (OBS) non-refractory PM<sub>1</sub> and modelled (MOD) non-refractory PM<sub>2.5</sub> at 10 AMS sites in Europe during February-March 2009. Mace head is reported only in Table 3 since the ammonium component is not available.

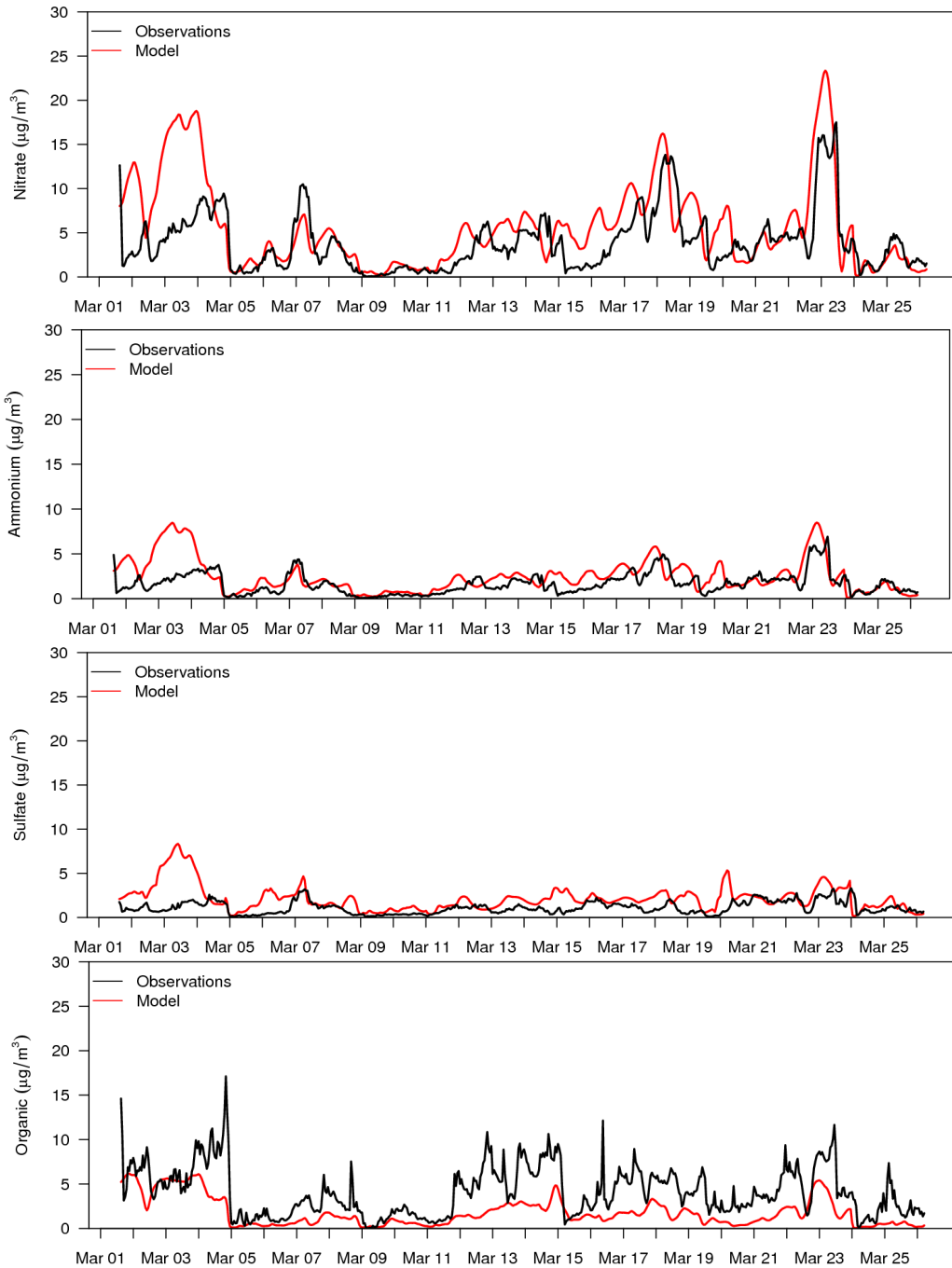


Figure 4. Comparison of observed and modelled nitrate, ammonium, sulfate and organic aerosol at Payerne for March 2009.

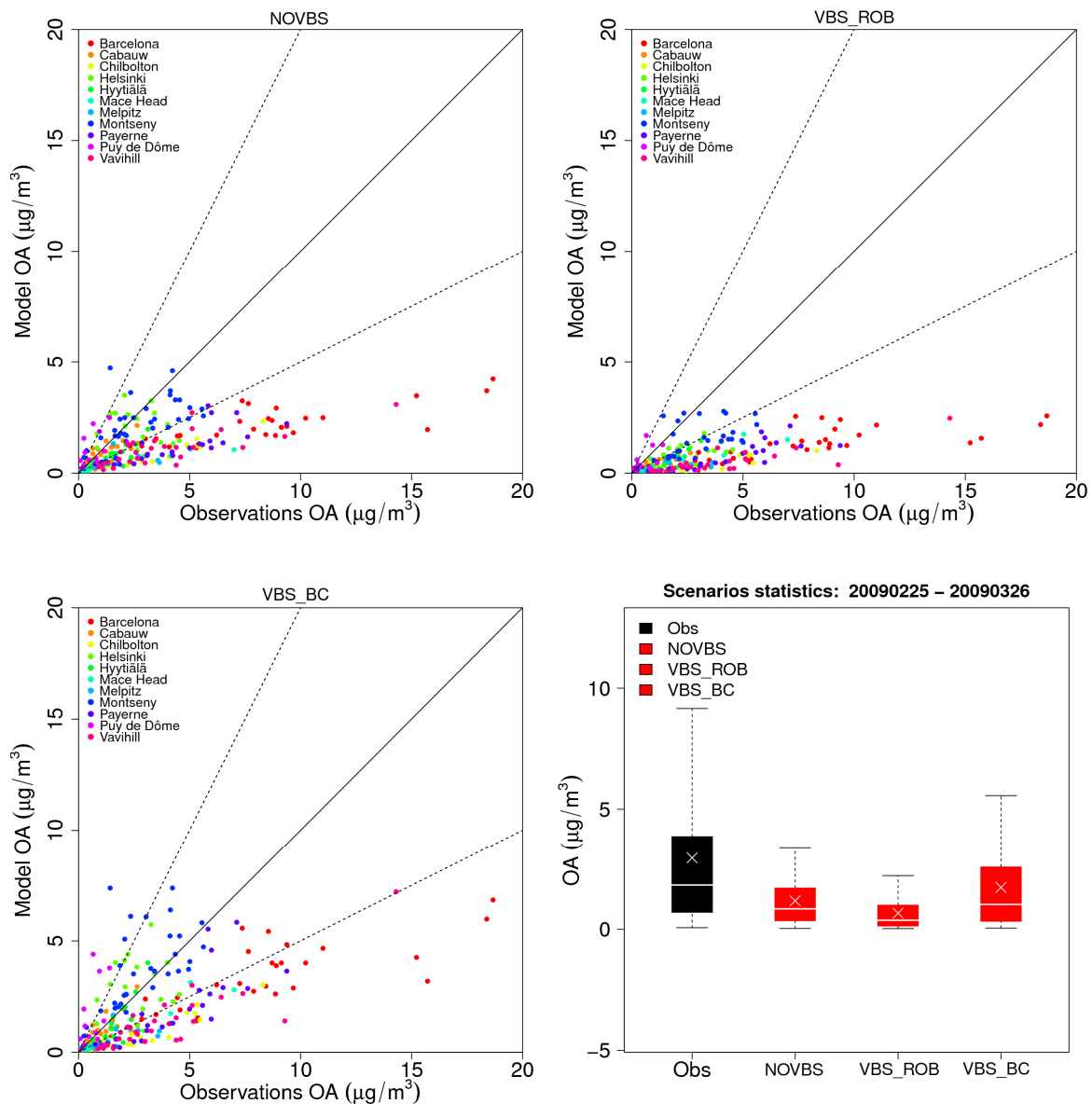


Figure 5. OA daily average scatter plots for NOVBS, VBS\_ROB and VBS\_BC scenarios for February-March 2009 for stations in Table 3. Solid lines indicate the 1:1 line. Dotted lines are the 1:2 and 2:1 lines. Boxplots indicate medians, 5<sup>th</sup>, 25<sup>th</sup>, 75<sup>th</sup> and 95<sup>th</sup> quantiles for observations (black) and sensitivity tests (red). The crosses represent the arithmetic means.  $R^2$  is 0.55 for NOVBS, 0.64 for VBS\_ROB and 0.59 for VBS\_BC (excluding the elevated sited of Puy de Dôme and Montseny).



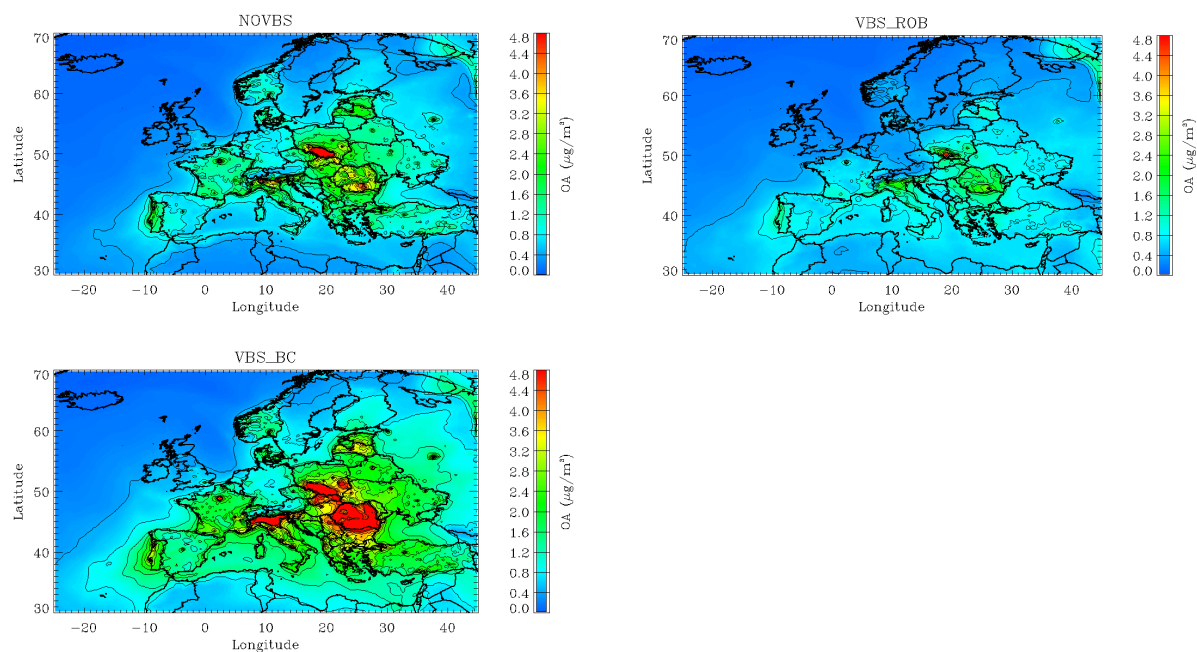


Figure 6. Predicted OA concentrations over Europe for the NOVBS, VBS\_ROB and VBS\_BC scenario in February-March 2009. Note that the color scale was limited to maximum of  $4.8 \mu\text{g}/\text{m}^3$  to facilitate comparison of the panels.

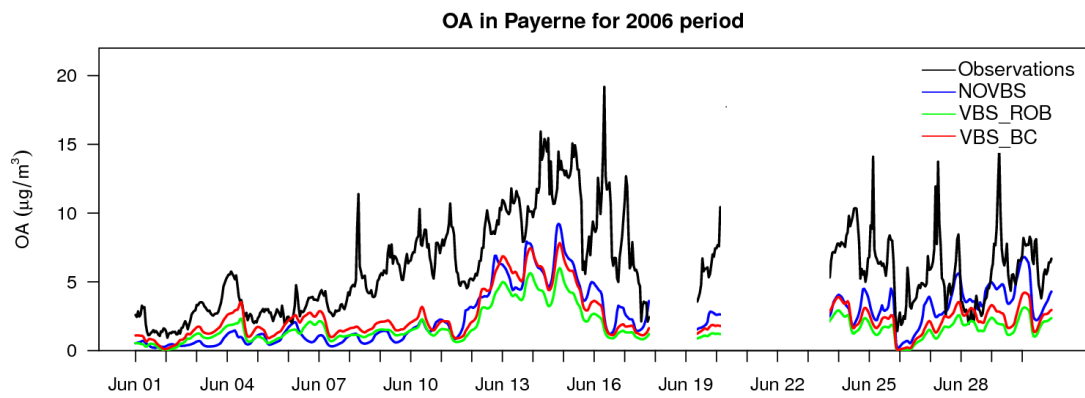
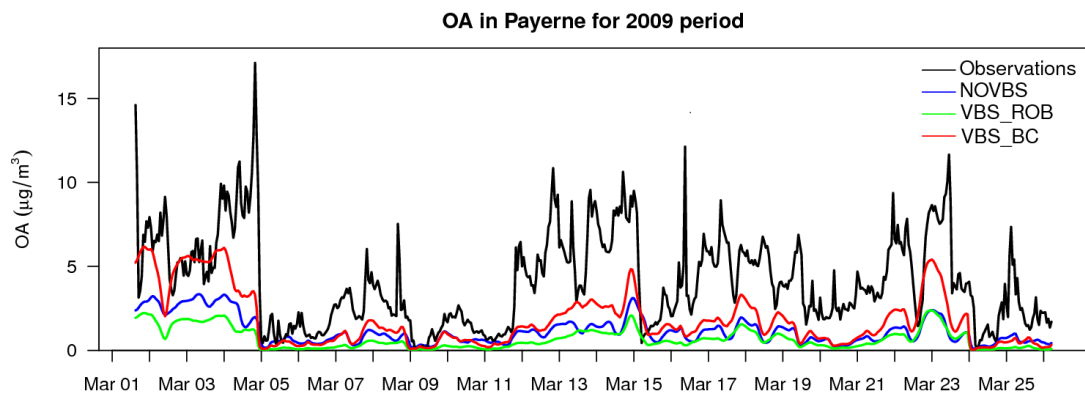


Figure 7. Predicted and observed total OA for scenarios NOVBS, VBS\_ROB and VBS\_BC in March 2009 (upper panel) and June 2006 (lower panel) at Payerne.

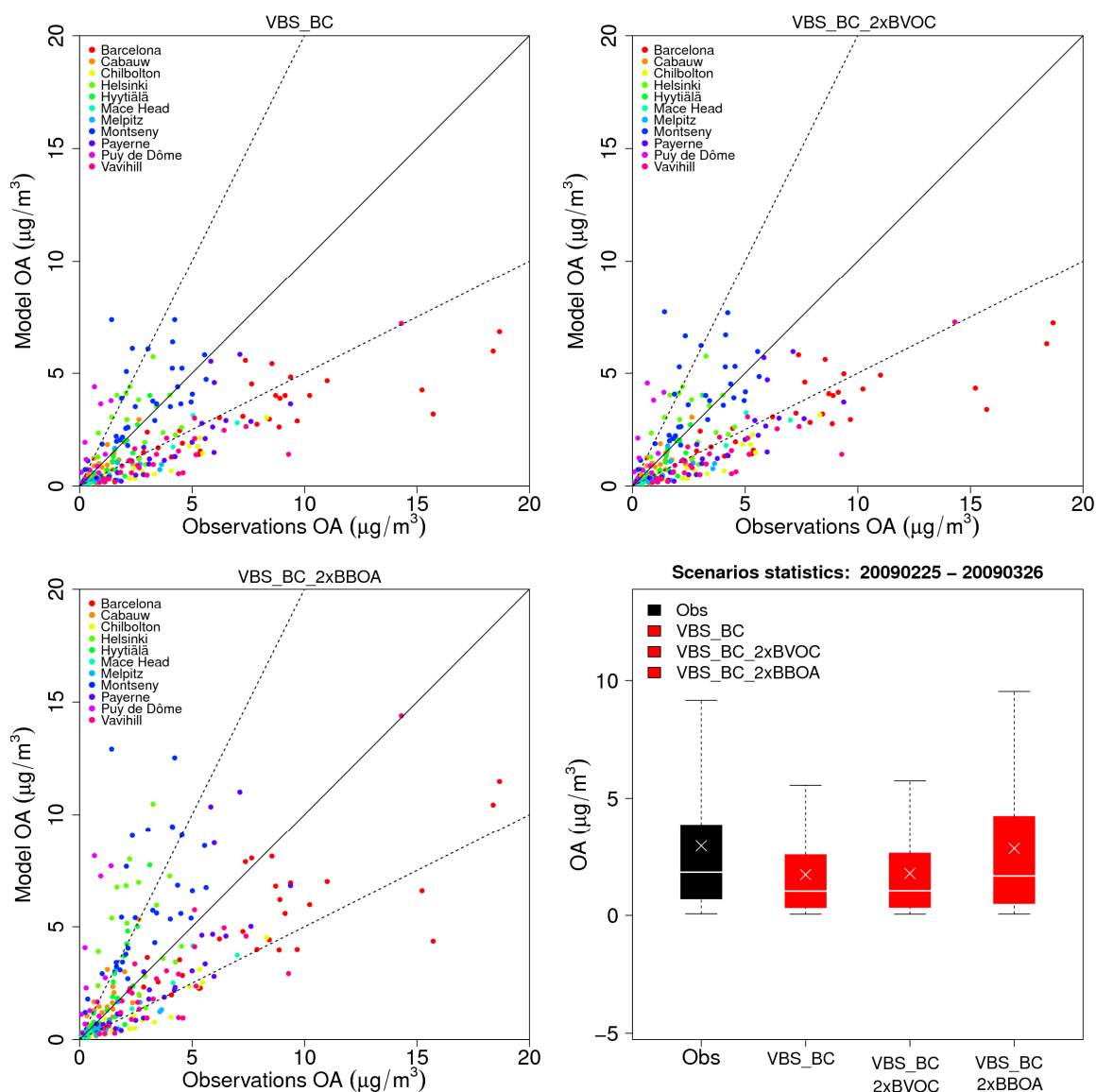


Figure 8. OA daily average scatter plots for VBS\_BC, VBS\_BC\_2xBVOC and VBS\_BC\_2xBBOA scenarios for February-March 2009 for stations in Table 3. Solid lines indicate the 1:1 line. Dotted lines are the 1:2 and 2:1 lines. Boxplots indicate medians, 5<sup>th</sup>, 25<sup>th</sup>, 75<sup>th</sup> and 95<sup>th</sup> quantiles for observations (black) and sensitivity tests (red). The crosses represent the arithmetic means.

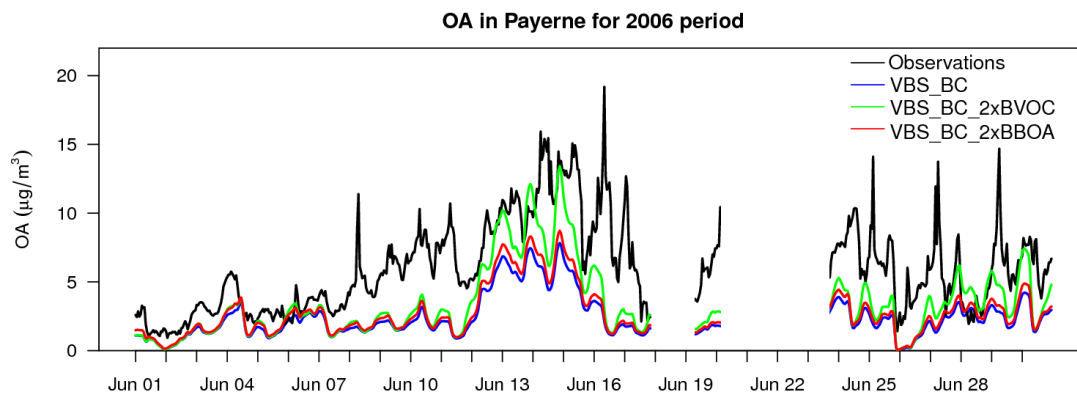
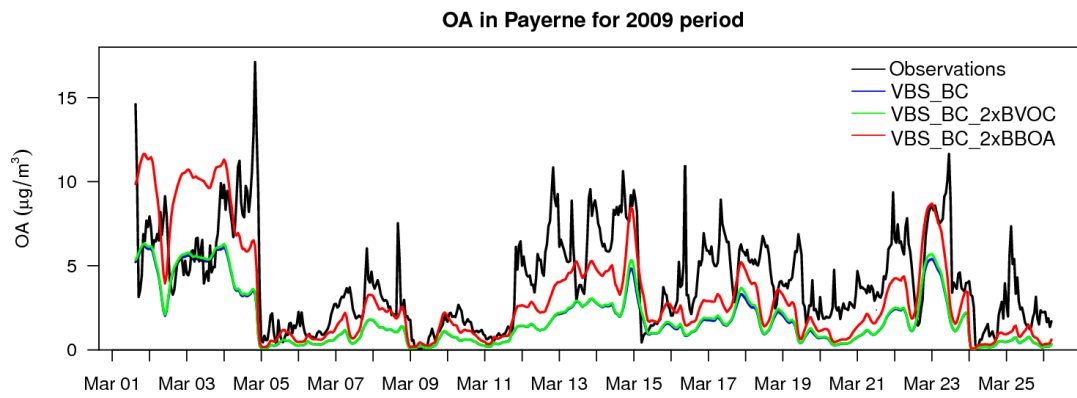


Figure 9. Predicted and observed total OA for scenarios VBS\_BC, VBS\_BC\_2xBVOC and VBS\_BC\_2xBBOA in March 2009 (upper panel) and June 2006 (lower panel) at Payerne.

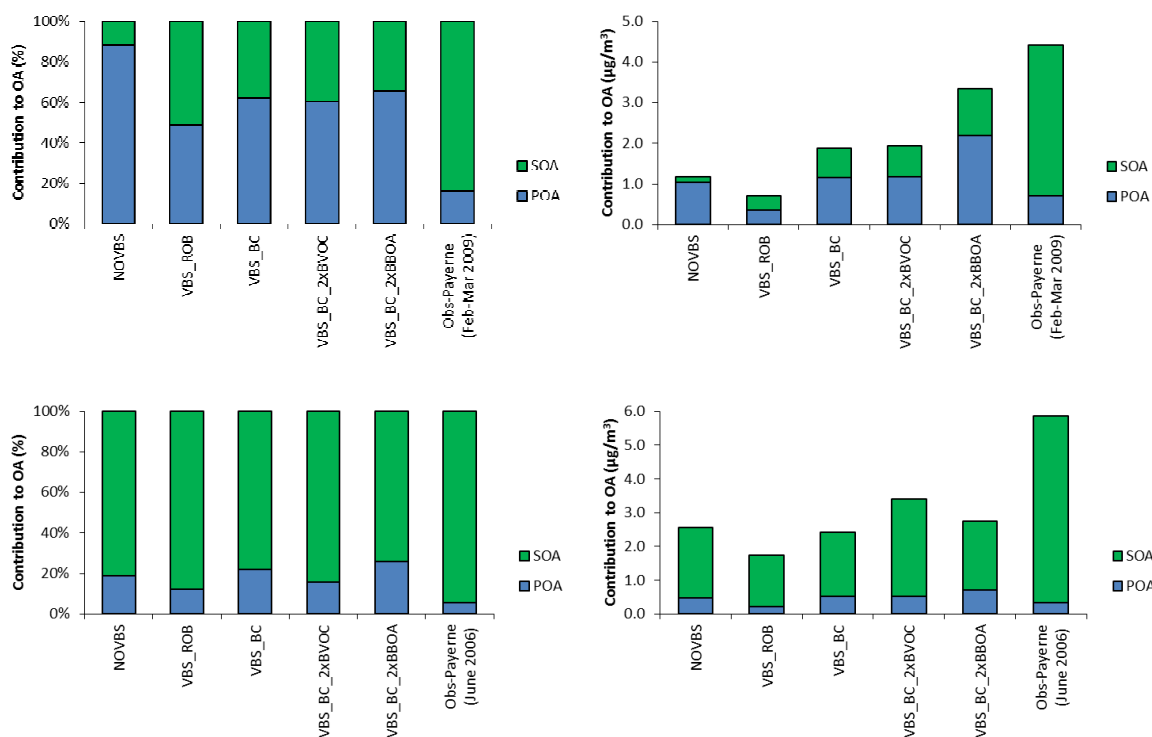


Figure 10. Relative (left) and absolute (right) contribution of predicted and measured POA and SOA fractions to the total OA mass at Payerne for February-March 2009 winter period (upper-panel) and June 2006 (lower-panel) and different model scenarios. NOVBS: (traditional non-volatile POA), VBS\_ROB (Robinson et al., 2007), VBS\_BC (Tsimpidi et al., 2010, Shrivastava et al., 2011), VBS\_BC\_2xBVOC (increased biogenic emissions relative to VBS\_BC), VBS\_BC\_2xBBOA (increased biomass burning emissions relative to VBS\_BC), Obs-Payerne: AMS-PMF.